Swift Machine Learning Model Serving Scheduling: A Region Based Reinforcement Learning Approach

Heyang Qin
University of Nevada, Reno
Reno, NV
heyang_qin@nevada.unr.edu

Syed Zawad
University of Nevada, Reno
Reno, NV
szawad@nevada.unr.edu

Yanqi Zhou
Google Brain
Mountain View, CA
yanqiz@google.com

Lei Yang
University of Nevada, Reno
Reno, NV
leiy@unr.edu

Dongfang Zhao
University of Nevada, Reno
Reno, NV
dzhao@unr.edu

Feng Yan
University of Nevada, Reno
Reno, NV
fyan@unr.edu

ABSTRACT

The success of machine learning has prospered Machine-Learning-as-a-Service (MLaaS) deploying trained machine learning (ML) models in cloud to provide low latency inference services at scale. To meet latency Service-Level-Objective (SLO), judicious parallelization at both request and operation levels is utterly important. However, existing ML systems (e.g., Tensorflow) and cloud ML serving platforms (e.g., SageMaker) are SLO-agnostic and rely on users to manually configure the parallelism. To provide low latency ML serving, this paper proposes a swift machine learning serving scheduling framework with a novel Region-based Reinforcement Learning (RRL) approach. RRL can efficiently identify the optimal parallelism configuration under different workloads by estimating performance of similar configurations with that of the known ones. We both theoretically and experimentally show that the RRL approach can outperform state-of-the-art approaches by finding near optimal solutions over 8 times faster while reducing inference latency up to 79.0% and reducing SLO violation up to 49.9%.

CCS CONCEPTS

• **Computing methodologies** → **Reinforcement learning**; • **Computer systems organization** → **Cloud computing**; • **Theory of computation**;

KEYWORDS

Model Inference, machine-learning-as-a-service (MLaaS), parallelism parameter tuning, reinforcement learning, workload scheduling, service-level-objective (SLO)

ACM Reference Format:
Heyang Qin, Syed Zawad, Yanqi Zhou, Lei Yang, Dongfang Zhao, and Feng Yan. 2019. Swift Machine Learning Model Serving Scheduling: A Region Based Reinforcement Learning Approach. In *The International Conference for High Performance Computing, Networking, Storage, and Analysis (SC '19), November 17–22, 2019, Denver, CO, USA.* ACM, New York, NY, USA, 14 pages. https://doi.org/10.1145/3295500.3356164

SC '19, November 17–22, 2019, Denver, CO, USA

ACM ISBN 978-1-4503-6229-0/19/11…$15.00
https://doi.org/10.1145/3295500.3356164

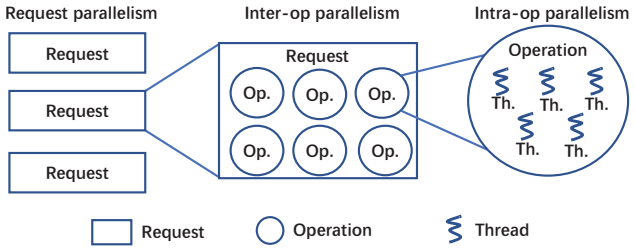

Figure 1: Different parallel computing implementation for machine learning serving on CPU.

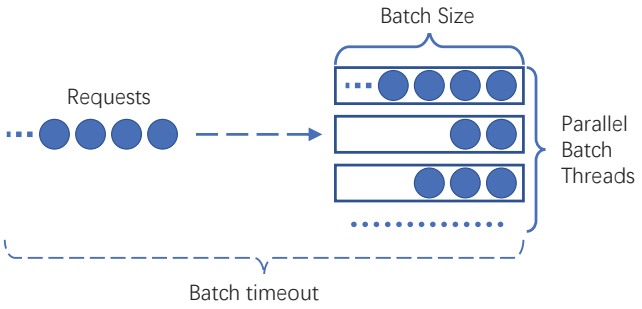

Figure 2: Configurations that can indirectly change the parallelism for machine learning serving on GPU.

1 INTRODUCTION

1.1 Motivation

Recent years have witnessed the success of machine learning in a variety of applications in areas of vision [17, 20, 35], speech [19, 24], and natural language [9]. Such success has prompted the development of Machine-Learning-as-a-Service (MLaaS) [49] that provides *model training* and *model inference* supports in the cloud. In the model training phase, ML models are crafted and trained using large amounts of data in an iterative manner. Then, the trained models are deployed in serving mode to provide various inference

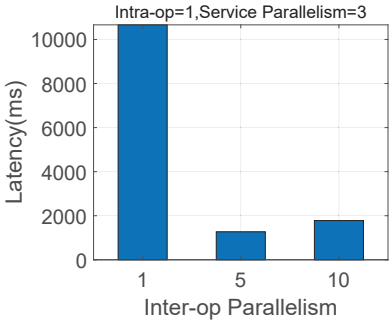

Figure 3: Tensorflow serving performance under different parallelism configurations for Inception V3 model running on CPU. Appropriate parallelism improves system performance yet excessive parallelism decreases it because of interference. This observation is consistent with previous study [69]. Experimental setup is detailed in Section 6.1.

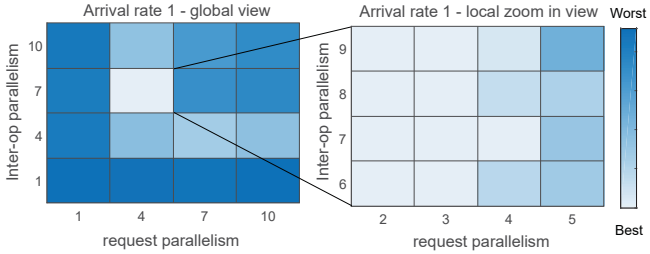

Figure 4: Latency under the arrival rate of 14 requests per second on CPU with different parallel configurations (intra-op parallelism is set to 10) using Inception V3 deployed in Tensorflow Serving. The lighter the color, the lower the latency. The left plot shows a global performance view of configurations and the right plot is the zoomed in view of the performance in a small region of configurations. The coarse-grained plot shows the latency is quite versatile globally while the zoomed-in fine-grained plot shows the latency is smooth locally (i.e., the neighboring points in the heatmap).

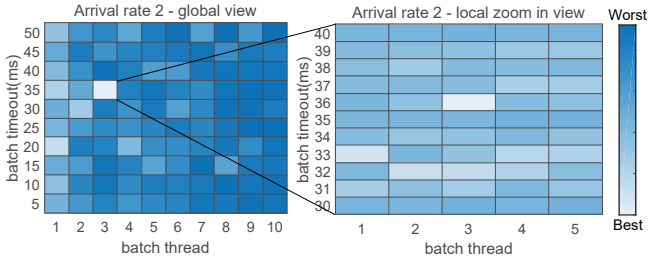

Figure 5: Latency under the arrival rate of 61 requests per second on GPU with different parallel configurations (batch size is set to 50) using Inception V3 model deployed in Tensorflow Serving. The lighter the color, the lower the latency. Left plot shows a global performance view of configurations and the right plot is the zoomed in view of the performance in a small region of configurations.

services, such as image classification [28], language processing and translation [39], photo search [50] and captioning [67], and drug discovery [48]. In this paper, we focus on providing low latency *model inference* (a.k.a machine learning serving). Compared with model training that targets at maximizing throughput (i.e., an offline process tries to iterate over all training samples as fast as possible, which may take hours or even days), one main requirement of machine learning serving is to achieve consistently low latency to attract and retain users (i.e., serves user requests in real-time). However, different from traditional serving applications, machine learning models with good performance for many challenging tasks are often containing billions of neural connections, and may take seconds or even minutes (due to both processing time and queuing waiting time) to fulfill users' requests [76] when executed in a *sequential* manner, resulting in unacceptably long latency or even making these applications non-shippable (due to latency SLO violation). However, typical SLOs of MLaaS in production system require 500-800ms [23, 69, 70, 74].

To satisfy the needs of MLaaS for meeting the low latency Service Level Objective (SLO), a natural and promising approach is to parallelize computation [17, 20]. Parallelization is especially useful for machine learning, because most underlying operations in these models are vector-matrix multiplications or matrix-matrix multiplications [13]. Running modern machine learning systems on CPU based infrastructure, parallelization usually have two levels [76]. At the request level, requests can be executed in parallel, which is noted as *request parallelism*. Each request is usually composed of many operations, so at the operation level, computation can be further parallelized as *inter-op parallelism* (multiple operations running simultaneously) and *intra-op parallelism* (each operation utilizes multiple threads). Fig. 1 illustrates these three parallel implementations. Hardware accelerator based infrastructure has its own parallelization configuration. We use GPU as an example in this paper, where the internal parallelism such as thread blocks and scheduling partitions are controlled by the hardware schedulers and are difficult to control directly through software-based approaches [64]. However, there are several user defined parameters that can indirectly impact the parallelization performed by GPU hardware scheduler. As shown in Fig. 2, the user defined Batch Size and Batch Timeout (i.e., maximum wait time allowed to form the target batch size) together determines the input dimensions, which impacts hardware scheduling decisions such as how the scheduler allocates and dispatches thread blocks and also how warp scheduler schedules warps into scheduling partitions. The Parallel Batch Threads can also impact the parallelism decisions of the GPU hardware scheduler. In machine learning serving systems, each parallel implementation and each related configuration becomes a control knob. Parallelism configuration has significant impact on system performance. As indicated in Fig. 3, a well-tuned parallelism configuration can boost system performance up to 10 times compared to sequential execution (e.g., running Inception V3 on CPU infrastructure).

Machine learning serving is usually interactive and latency sensitive [23, 69] compared with model training or HPC workload which is usually throughput-oriented (i.e., SLO-agnostic). Compared with traditional web service, ML-serving usually involves hundreds to thousands of operations with complex correlation among them [5], which makes it challenging to model in a white-box manner. This makes machine learning serving an unique workload that is challenging to breakdown and do fine-tuning at operation level. How to

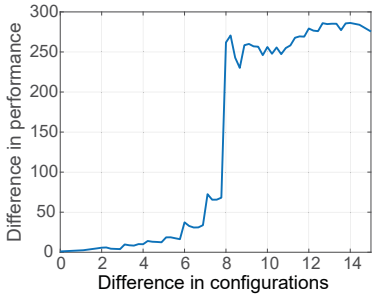

Figure 6: Difference in performance v.s. difference in configuration. The difference in configurations is calculated by their Euclidean distance.

optimally control these knobs depends on the performance requirement, workload characteristic, and available computing resources, which becomes an important yet challenging problem.

Parallelism configuration tuning has recently garnered much attention [7, 30]. However, existing methods require domain specific information and techniques to tune the parallelism configuration (see the detailed discussion in Section 2), which may not be applicable to many machine learning applications. Recently, Feng *et al.* proposed SERF in [69, 70] to achieve optimal parallelism configuration for machine learning serving using an analytical queuing model, which is applicable for exponential arrival process and homogeneous request size in certain image classification applications. For many other applications (such as video, speech, and natural language processing), the arrival process may not be exponential, and request sizes may be heterogeneous. In addition, SERF supports only request level parallelism and CPU-based hardware. Therefore, there is a pressing need to develop a novel approach that can support two levels of parallelisms and hardware accelerators like GPU to effectively and efficiently tune parallelism configuration for machine learning applications with diverse arrival processes and heterogeneous request sizes.

1.2 Challenges

It is challenging to tune parallelism configuration in modern machine learning serving systems. For CPU-based infrastructure, the configuration space is relatively large due to the two-level parallelism. Fig. 4 illustrates request latency under only two parallelism configurations with fixed intra-op parallelism. Even for two parallelisms on a machine with only 10 cores, there are many parallelism configurations. The similar observation holds for GPU-based infrastructure, see Fig 5. For GPU, the search space is even larger due to the wider range of configuration parameters (e.g., Batch Timeout alone can have hundreds to thousands possible choices). In addition, due to the indirect impact of configuration parameters in the GPU case, it is very difficult to model or predict the behaviors. Worse still, the optimal parallelism configuration is also very sensitive to the load. In Fig. 4, even with a slight change in load, the latency distribution (note the latency here is composed of both service time and queuing waiting time) under different parallelism configurations becomes quite different, which significantly increases the search space and prohibits exhaustive search. Moreover, it is worth noting that the high computation and memory needs of machine learning models can result in complex interference behavior among parallel computation [69, 70], which is less a problem in model training that focuses on the overall throughput rather than the processing speed of individual request. Such non-linear performance behavior of different configurations brings significant challenges for profiling and analytical modeling [36, 71].

In addition, modern machine learning models usually contain thousands to tens of thousands of operations with complex dependencies, which may result in the state-of-the-art modeling techniques [69, 70] ineffective. Moreover, the workload and system environment in many machine learning applications are often highly dynamic [16, 73], which requires the scheduling policy with an agile adaptive ability, in order to meet the sensitive latency SLO [23, 42]. In this case, traditional learning-based methods [36], requiring a large training set and a long convergence time, can hardly be applicable to machine learning model serving. Therefore, swift deployment is required for most online serving systems, which can learn the dynamics of the workload and system environment and optimize the model performance in an online manner.

1.3 Summary of Main Contributions

In this paper, we propose a swift machine learning serving scheduling framework to solve the above challenges. The proposed framework is driven by a lightweight region-based reinforcement learning (RRL) approach that can efficiently identify the optimal configuration under different workloads. Like previous studies [32, 45], we formulate our problem as Markov Decision Process. The key insight is that the system performances under different similar configurations in a region can be accurately estimated by using the system performance under one of these configurations, due to their similarity (see Fig. 6). This key finding motivates us to develop RRL that can speedup the learning process by orders of magnitude faster than state-of-the-art deep reinforcement learning methods with very limited training data. We theoretically show that this speedup increases with the size of the region, which, however, would result in a performance gap between the RRL and the optimal solution due to the estimation error. Thanks to the unique structure of our problem (see Fig. 6), we are able to choose a suitable size of the region such that the learning speed can be significantly improved with near optimal performance.

We prototype the proposed framework on top of the popular Tensorflow Serving [44] machine learning serving system and support both CPU and GPU based hardware infrastructure. We release the source code for public access.[1] We conduct extensive experimental evaluations on both CPU and GPU clusters and the results show that by continuously learning the new traffic patterns and updating the scheduling policies, RRL can quickly adapt to the ever-changing dynamics of workloads and system environments. Compared to the state-of-the-art reinforcement learning methods, RRL can reduce the average latency up to 79.0% on CPU-based infrastructure and up to 69.3% on GPU-based infrastructure compared to state-of-the-art approaches DeepRM[38] and CAPES[37]. In the SLO-aware scenario, RRL can offer SLO guarantee even under strict targets and provide up to 49.9% SLO violation reduction compared to CAPES and up to 43.4% compared to DeepRM. In addition, the proposed

[1] https://github.com/SC-RRL/RRL

framework does not have assumptions on workload or underlying systems and thus can be used for most modern machine learning systems and applications.

2 BACKGROUND AND RELATED WORK

2.1 Machine Learning Serving

Machine learning has recently shown a great success on important yet challenging artificial intelligence applications, such as vision, speech, and natural language. How to efficiently deploy trained machine learning models in serving (or sometimes called inference or model serving) mode to provide low latency services has drawn great attention in both academia and industry [18, 69, 70, 75]. Major public cloud service providers like Google, Amazon, and Microsoft all provide MLaaS to facilitate users to publish their models and provide online services. Several machine learning serving systems have been open-sourced recently [10, 18, 44], among which the most widely used one is Tensorflow Serving [44]. In this paper, we use Tensorflow Serving as a case study system to implement and evaluate the proposed framework.

Hardware acceleration [14, 46] has been used to accelerate the computation in machine learning serving by using customized hardware such as GPUs, FPGAs, and ASICs. Software techniques such as model compression and simplification [27] have also successfully improved the latency of machine learning serving through reducing computation time and storage space by trading off some accuracy. In addition, recent work using compiler techniques [3] and acceleration library [1] have also shown good results in accelerating machine learning serving. All the above techniques are complementary to our scheduling framework and can be combined with our work to achieve better results as all of them use parallelization techniques and have tuning parameters for optimal performance. In addition, the proposed framework does not rely on any specific models or underlying systems or hardware.

Another promising technique for reducing the latency of machine learning serving is parallelism as most operations in machine learning models are vector-matrix multiplications or matrix-matrix multiplications [13] that can be efficiently parallelized. *Request parallelism*, *inter-op parallelism*, and *intra-op parallelism* are the typical ways to parallel computation on CPU in today's machine learning serving systems. On GPU, computation is parallelized through SMs and scheduling partitions, though difficult to control through software mechanisms, it can be indirectly adjusted through batching parameters such as *batch size*, *batch threads*, and *batch timeout*. To achieve efficient parallelism, it is critical to understand the behavior of different configurations. As discussed in the introduction, existing methods [7, 15, 30, 69, 70] either require domain specific information and techniques to tune the parallelism configuration or are applicable for special arrival process with homogeneous request size in certain applications. To achieve a more general solution, we aim to design a scheduling framework that can work with general user traffic patterns and system environments on both CPUs and GPUs based infrastructure.

2.2 Interactive Serving

Machine learning serving is not the first application utilizing parallelism to reduce latency. Actually, parallelism has been widely used in many online services for the similar purpose. Here we focus on interactive serving systems that utilize parallelism to accelerate processing or share resources among users' requests. There is a line of work in the literature studying adaptive resource allocation for requests sharing the same server systems [25, 47]. However, they consider only request level parallelism. Raman *et al.* develop an API and runtime system for parallelism orchestration [47], but they assume requests do not interfere with each other, which does not hold for computation-intensive machine learning serving. Haque *et al.* observe large variability on interactive services and propose incremental parallelization approach to achieve optimal latency [25], which is not suitable for machine learning serving workload due to the large number of operations and complex dependencies. Another line of work [7, 15, 30] relies on domain knowledge of specific applications and/or the special architecture of specific systems to guide the optimization of parallel configurations. Dazhao *et al.* design an adaptive scheduling for Spark Streaming [15]. Jeon *et al.* propose an analytical algorithm to compute the optimal parallelism based on their characterization results of web search queries [30]. Alipourfard *et al.* build performance models using Bayesian Optimization for cloud configuration with the focus of recurring big data analytics [7]. None of these work investigates the unique characteristics of machine learning workloads and tailor the parallelism scheduling methodology accordingly.

2.3 Parameter Tuning using Reinforcement Learning

Reinforcement learning [22, 56, 59, 68] was first proposed in 1940s and has been widely used in different applications. Here we focus on the application of system parameter tuning using reinforcement learning. Mao *et al.* propose reinforcement learning based resource management method for multi-resource cluster scheduling problem [38]. Li *et al.* develop a reinforcement learning based parameter tuning system for storage systems [37]. Both work use traditional point-based reinforcement learning and suffer from slow convergence and adaptivity. Mirhoseini *et al.* propose to optimize Tensorflow operation placement between CPU and GPU using long short-term memory (LSTM), which is applicable for only CPU-GPU co-design architecture [41]. In this paper, we develop a new region-based reinforcement learning based on the unique characteristics of machine learning serving performance behavior to significantly improve the convergence speed and the agility in dynamic environment.

2.4 Workload Scheduling

Many works have studied the job scheduling problem in HPC cluster. Baskaran *et al.* [12] proposed a model based parameter tuning method for applications across GPUs. Isaila *et al.* [29] proposed a heuristic algorithm to schedule I/O parallel jobs in a decentralized manner for filesystems. Krishnamoorthy *et al.* [34] proposed a framework that can automatically optimize application memory placement in parallel systems by block-sparse arrays. In the record-breaking HPC cluster built by Sakagami *et al.* [53], the parallelism is manually tuned. For ML-serving, different serving models, workloads, and system environments can lead to very different performance characteristics. Thus the approaches of modeling, heuristic and white-box tuning are infeasible for machine learning serving.

3 RRL-BASED SCHEDULING FRAMEWORK

In this section, we present the RRL-based scheduling framework for machine learning serving. The RRL-based scheduling framework is designed to dynamically adjust the parallelism configuration of machine learning serving systems based on dynamic system load, in order to optimize system performance (e.g., response latency or resource consumption). As illustrated in Fig. 4, system performance varies under different parallelism configurations even for the same load, and the relationship among the system performance, parallelism configurations, and system load is challenging to capture in a closed form. To tackle this challenge, the proposed framework leverages a learning approach to find the optimal parallelism configuration. Specifically, the proposed framework consists of three main components: 1) profiler, 2) scheduler, and 3) region-based reinforcement learning, as illustrated in Fig. 7. The profiler collects various system characteristics, such as the current user traffic load and the corresponding system performance (e.g., average latency or resource consumption) under this load and the present parallelism configuration. The scheduler then adjusts the parallelism configuration for the measured load level based on the current scheduling policy. At the same time, the region-based reinforcement learning dynamically updates the scheduling policy based on the measured system load and corresponding performance, in order to adapt to the system dynamics.

1) Profiler. The profiler measures the system load (i.e., request arrival rate) and the latency (also known as response time) of each request. Latency is used to measure the system performance. Meanwhile, the profiler also collects hardware-related information (such as CPU core number, CPU utilization, available GPUs, GPU utilization, and network statistics). All these information can be used to optimize the system performance for a specific scheduling objective.

2) Scheduler. The scheduler adjusts the parallelism configuration based on the current system load, scheduling policies, and hardware information such as the availability of resource.

3) Region-based reinforcement learning. As the core of the proposed framework, the region-based reinforcement learning component aims to find the optimal scheduling policy and quickly adjust the scheduling policy to adapt to the system dynamics. Specifically, the reward function in Fig. 7 first calculates the value of the system objective function using the system performance measured by the profiler, and then the learning component learns the scheduling policy based on this observed reward. One key challenge is that the learning process would be significantly long if the scheduling policy is incrementally improved in a point-by-point learning manner. To address this challenge, the proposed region-based reinforcement learning can speedup this learning process by leveraging the key feature of the system as illustrated in Fig. 6. It is observed that the system performances under different similar configurations are similar. Based on this feature, the system performance under one configuration can be used to estimate the system performances under other similar configurations, which would significantly reduce the number of samples needed to learn the optimal scheduling policy. For example, if we choose the radius of the configuration region equal to 2, then we can use a single observation to update all configurations in this region and obtain a roughly 10 times faster convergence with limited performance loss due to the estimation error. The detailed design is presented in Section 4.

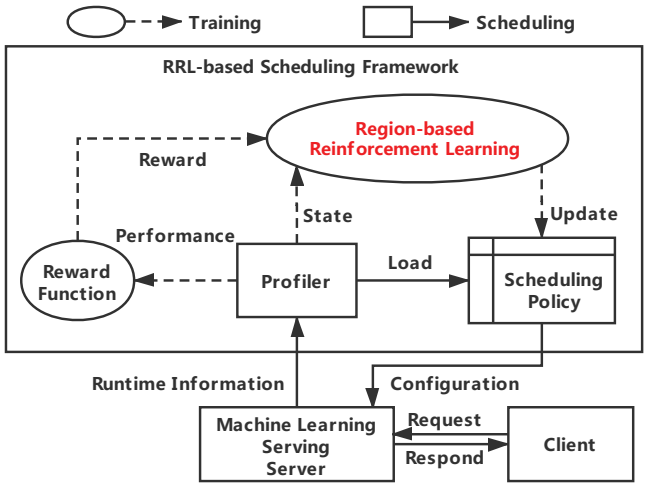

Figure 7: Overview of RRL-based scheduling framework.

4 REGION-BASED REINFORCEMENT LEARNING

In this section, we propose a region-based reinforcement learning (RRL) approach, in order to speedup the learning process of the scheduling policy. Specifically, we first formulate the machine learning serving scheduling as a Markov Decision Process (MDP), and then theoretically show that the RRL approach can achieve a near optimal solution with fast convergence speed.

4.1 ML Serving Scheduling: A MDP View

The objectives of machine learning serving scheduling are 1) to minimize response latency using a given amount of resources [31, 47] or 2) to minimize resource consumption while meeting latency SLO. Both objectives are supported in our scheduling framework [40, 77]. In the interest of space, we focus on the first objective of minimizing response latency.

Let $s \quad \mathcal{S}$ denote the overall load level (i.e., system state), where $\mathcal{S}$ denotes the set of possible load levels. The parallelism configuration (i.e., system action) $c \quad C$ is denoted as a tuple of request parallelism c^{service}, inter-op parallelism c^{inter}, and intra-op parallelism c^{intra}, i.e., $c = c^{\text{service}}, c^{\text{inter}}, c^{\text{intra}}$, where C denotes the set of possible parallelism configurations. For machine learning serving, latency can vary under different loads (system states) for the same parallelism configuration [69], which is challenging to characterize in a closed form. However, the average request latency $r\ s, c$ under the system state s and the parallelism configuration c can be measured as reward. In this paper, we assume that the scheduler has no apriori knowledge of system state transitions, except the Markov property (i.e., the state transition depends on only the previous state)[2]. Under this model, the machine learning serving scheduling is cast as a Markov Decision Process, aiming to minimize

[2]Markov models are often used to model the workload dynamics, e.g., [45] verifies the Markov property for different applications. In our application, the Markov property

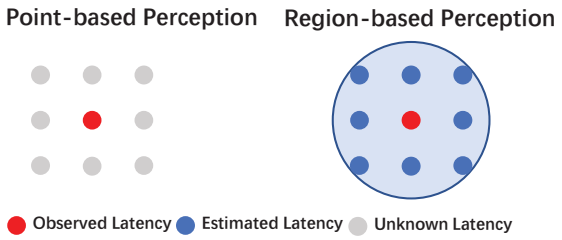

Figure 8: Point-based vs. region-based learning. The RRL approach can more efficiently learn the latency under different configurations.

the expected cumulative discounted latency $\mathbb{E}\left[\sum_{t=0} \gamma^t r_t\ s_t, c_t\ \right]$, where $\gamma \quad 0,1$ is a discount factor and $r_t\ s_t, c_t$ denotes the latency observed at time t under system state s_t and parallelism configuration c_t.

At each time t, the scheduler chooses a parallelism configuration based on a policy, defined as $\pi : \pi\ s, c \quad 0,1$, where $\pi\ s, c$ is the probability that configuration c is used in state s. To find the optimal policy, the Q-learning method can be applied. However, the convergence of the Q-learning method is slow, especially when the space of state-configuration pairs is large. One key reason for this slow convergence is that it searches the space point by point and incrementally improving the policy. Though many approaches [11, 21, 63] have been proposed to improve the convergence speed, they are still *point-based* learning essentially, and would not be applicable to our problem with large state-configuration space as shown in our experiments in Section 6.

4.2 RRL: From Point-based to Region-based Learning

To speedup the learning process, we propose the RRL approach. *The key idea is that when observing the latency $r\ s, c$, we will estimate the latency in a region with configurations close to c under this state s, and then use the estimated latency in this region to learn the policy, as illustrated in Fig. 8.* Intuitively, this region-based learning approach would significantly improve the learning speed if a large region is used. However, the converged policy may deviate from the optimal one, due to the potential estimation errors of the latency associated with the region such that the larger the region is, the larger the potential errors would be. Obviously, there is a trade-off between the learning speed and the optimality of the policy, which intimately depends on the size of the region and the latency estimation scheme. When the region degenerates to a single point, the RRL approach would degenerate to the traditional reinforcement learning approaches. In this paper, Euclidean distance is used to measure the distance between two configurations since both CPU and GPU configurations are numeric, see Fig. 9. Note that other similarity measures can also be applied in RRL.

Specifically, the RRL approach consists of two main components: 1) latency estimation based perception and 2) policy update.

4.2.1 Latency estimation based perception. Let $Q_t\ s_t, c_t$ denote the perception of the expected cumulative discounted latency under state s_t and configuration c_t. Define the region around c_t as $C\ c_t = c\ \ c - c_t \quad \delta, \forall c \quad C$, where $\delta \quad 0$ denotes the size of the region. Using the observed latency $r_t\ s_t, c_t$, the latency under other configurations in $C\ c_t$ can be estimated as

$$\hat{r}_t\ s_t, c = f\ c, r_t\ s_t, c_t\ , \forall c \quad C\ c_t\ , \tag{1}$$

where $f : C \quad \mathbb{R}^+ \quad \mathbb{R}^+$ is the latency estimation function and $f\ c_t, r_t\ s_t, c_t = r_t\ s_t, c_t$. Based on (1), we update the perception of the expected cumulative discounted latency in the region by

$$\forall c \quad C\ c_t\ ,\ Q_{t+1}\ s_t, c \quad = \quad 1-\alpha_t\ Q_t\ \ s_t, c\ + \alpha_t\ \hat{r}_t\ s_t, c \\ +\gamma \min_{\tilde{c}\ \ C} Q_t\ s_{t+1}, \tilde{c}\ , \tag{2}$$

where $\alpha_t \quad 0,1$ is the learning rate. As is standard, the learning rate is assumed to satisfy $\sum_{t=1} \alpha_t = \quad$ and $\sum_{t=1} \alpha_t^2 < \quad$. The perceptions of other configurations ($c \notin C\ c_t$) will remain the same, i.e., $Q_{t+1}\ s_t, c = Q_t\ s_t, c\ , \forall c \notin C\ c_t$.

4.2.2 Policy update. Based on the perceptions, we can use the Boltzmann distribution [4] to update the policy for state s_t

$$\pi_t\ s_t, c = \frac{\exp\ -\beta Q_t\ s_t, c}{\sum_{\hat{c}\ \ C} \exp\ -\beta Q_t\ s_t, \hat{c}}, \forall c \quad C, \tag{3}$$

where $\beta \quad 0$ controls the exploration-exploitation trade-off. When β is very small, the scheduler would explore the space randomly; when β is large, the scheduler would tend to exploit the configuration with the lowest perceived latency.

It is worth noting that the performance of the RRL approach hinges on the accuracy of the latency estimation (1). In practice, it is challenging to characterize f in a closed form, due to the stochastic nature of the state and the latency. To tackle this challenge, we implement this estimation function using neural network as discussed in Section 5. The detailed description of the RRL approach is given in Algorithm 1.

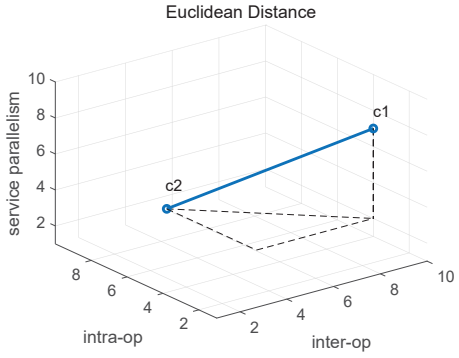

Figure 9: An example of Euclidean distance between two configurations c_1 and c_2, i.e., $\sqrt{c_1^{\text{service}} - c_2^{\text{service}\ 2} + c_1^{\text{inter}} - c_2^{\text{inter}\ 2} + c_1^{\text{intra}} - c_2^{\text{intra}\ 2}}$.

4.3 Performance Analysis of RRL

In this section, we will analyze the convergence rate and optimality performance of the RRL approach. To facilitate the analysis, we assume that the estimation error of the latency estimation (1) is upper bounded by $\Delta \quad 0$ for all state-configuration pairs in the

is also satisfied. The experiments in Section 6 also corroborate the correctness of the Markov model in our application.

Algorithm 1 Region-based reinforcement learning

Initialization: Choose β, δ, and γ. Set $t = 0$ and $Q_0(s,c) = 1\bullet C$, $\forall c \in C, s \in \mathcal{S}$.
For each time slot t
1) Choose a configuration based on the current policy π_t.
2) Update the perception based on (2).
3) Update the policy for the current state s_t based on (3).

space, i.e.,

$$\hat{r}_t(s_t,c) \in r_t(s_t,c) \pm \Delta, \forall c \in C(c_t), s_t \in \mathcal{S}, \tag{4}$$

where $r_t(s_t,c)$ denotes the real latency that can be observed if the configuration c is chosen. In (4), Δ is intimately related to the size of the region δ. In general, Δ increases with δ, and Δ becomes zero when δ is zero.[3] The main results are summarized in the following theorem.

Theorem 4.1. *The RRL approach can asymptotically converge to a near optimal solution with probability one as t goes to infinity. The performance gap is upper bounded by $\frac{\Delta}{1-R}$. The asymptotic convergence rate is $O\left(1\bullet n_{\boxtimes} t^{R-1}\right)$ if $R \in (0, 1\bullet 2)$ and $O\left(\sqrt{\log\log n_{\boxtimes} t \bullet n_{\boxtimes} t}\right)$ otherwise, where $n_{\boxtimes}$ denotes the number of state-configuration pairs in the region with size δ and R denotes the ratio of the minimum and maximum state-configuration selection probabilities.*

Proof. First, we introduce an auxiliary perception process $\hat{Q}_t(s_t,c_t)$ as follows:

$$\begin{aligned}\hat{Q}_{t+1}(s_t,c_t) = {} & (1-\alpha_t)\hat{Q}_t(s_t,c_t) + \alpha_t r_t(s_t,c_t) \\ & + \gamma \min_{\tilde{c} \in C} Q_t(s_{t+1},\tilde{c}),\end{aligned} \tag{5}$$

where $\hat{Q}_t(s_t,c_t)$ corresponds to the learning process using the real latency instead of the estimation (1). Then, the performance results of the RRL approach can be obtained by comparing $Q_t(s_t,c_t)$ with the optimal $Q^*(s_t,c_t)$ using $\hat{Q}_t(s_t,c_t)$. The idea is to use triangle inequality to decompose the comparison of $Q_t(s_t,c_t)$ and $Q^*(s_t,c_t)$ into two difference processes:

$$\begin{aligned}& Q_t(s_t,c_t) - Q^*(s_t,c_t) \le Q_t(s_t,c_t) - \hat{Q}_t(s_t,c_t) \\ & + \hat{Q}_t(s_t,c_t) - Q^*(s_t,c_t).\end{aligned} \tag{6}$$

Using stochastic-approximation techniques and prior convergence results of traditional Q-learning [62], we can obtain the upper bounds for each difference process in (6), which are summarized in the following lemmas.

Lemma 4.2. *For each time t, the difference process of $Q_t(s_t,c_t)$ and $\hat{Q}_t(s_t,c_t)$ satisfies $Q_t(s_t,c_t) - \hat{Q}_t(s_t,c_t) \le \frac{1}{1-R}\Delta$.*

Proof. We show $Q_t(s_t,c_t) - \hat{Q}_t(s_t,c_t) \le \frac{1}{1-R}\Delta$ by induction. At $t = 1$, with assumption (4) for any $s \in \mathcal{S}$ and $c \in C$, we have

$$\begin{aligned}\hat{Q}_1(s,c) - Q_1(s,c) &= \alpha_0\hat{r}_0(s,c) - \alpha_0 r_0(s,c) \\ &\le \hat{r}_0(s,c) - r_0(s,c) \le \Delta = b_1\Delta,\end{aligned}$$

where $\alpha_0 = 1$, and $b_1 = 1$ is less than $1\bullet 1-\gamma$ where $\gamma < 1$.

[3] Note that Δ also highly depends on the accuracy of the estimation function. In this paper, a neural network based estimation function is implemented, and the error bound is shown to be small in our experiments.

Using induction, we assume that for a given $t > 1$,

$$\hat{Q}_t(s,c) - Q_t(s,c) \le b_t\Delta$$

for any $s \in \mathcal{S}$ and $c \in C$ holds, i.e., $b_t \le 1\bullet 1-\gamma$.

We aim to show that $b_{t+1} \le 1\bullet 1-\gamma$. At $t+1$, we have

$$\begin{aligned}& \hat{Q}_{t+1}(s_t,c_t) - Q_{t+1}(s_t,c_t) \\ &= (1-\alpha_t)\left(\hat{Q}_t(s_t,c_t) - Q_t(s_t,c_t)\right) + \alpha_t\left(\hat{r}_t(s_t,c_t) - r_t(s_t,c_t)\right) \\ &\quad + \gamma\left(\min_{c \in C}\hat{Q}_t(s_{t+1},c) - \min_{c \in C} Q_t(s_{t+1},c)\right) \\ &\overset{a}{\le} (1-\alpha_t)\left(\hat{Q}_t(s,c) - Q_t(s,c)\right) + \alpha_t\left(\hat{r}_t(s,c) - r_t(s,c)\right) \\ &\quad + \gamma\max_{c \in C}\left(\hat{Q}_t(s_{t+1},c) - Q_t(s_{t+1},c)\right) \\ &\overset{b}{\le} (1-\alpha_t)b_t\Delta + \alpha_t\Delta + \gamma b_t\Delta \\ &\overset{c}{\le} \left(1-\frac{1}{t}\right)b_t\Delta + \frac{1}{t}\Delta + \gamma b_t\Delta = b_{t+1}\Delta,\end{aligned}$$

where (a) we apply triangle inequality and use the fact $\min \hat{Q}_t(s_{t+1},c) - \min Q_t(s_{t+1},c) \le \max\left(\hat{Q}_t(s_{t+1},c) - Q_t(s_{t+1},c)\right)$. (b) We use the assumption that $\hat{Q}_t(s,c) - Q_t(s,c) \le b_t\Delta$ for any $s \in \mathcal{S}$ and $c \in C$. (c) After some algebra, we have the coefficient of α_t equal to $\Delta(1-b_t(1-\gamma))$, which is positive as $b_t \le 1\bullet 1-\gamma$. Thus, it holds for some $\alpha_t \le \frac{1}{t}$ that satisfies the conditions of the learning rate.

Therefore, we have a recurrence relation

$$b_{t+1} = \left(1-\frac{1}{t}\right)b_t + \frac{1}{t}(1+\gamma b_t).$$

By some algebra, we have the following recurrence equation:

$$b_{t+1} = \left(1+\frac{\gamma-1}{t}\right)b_t + \frac{1}{t}, b_1 = 1. \tag{7}$$

We can solve this recurrence equation and obtain the following solution

$$b_{t+1} = \frac{1}{\frac{\boxtimes(t+\boxtimes)}{\boxtimes(t+1\boxtimes\boxtimes)}(1-\gamma)}, \tag{8}$$

where $\boxtimes$ in (8) denotes the gamma function. Note that the right hand side of (8) is a non-decreasing function of t upper bounded by $\frac{1}{1-R}$, i.e.,

$$b_{t+1} = \frac{1}{\frac{\boxtimes(t+\boxtimes)}{\boxtimes(t+1\boxtimes\boxtimes)}(1-\gamma)} \le \frac{1}{1-\gamma}. \tag{9}$$

Thus, we have

$$\hat{Q}_t(s,c) - Q_t(s,c) \le b_t\Delta \le \frac{1}{1-\gamma}\Delta, \tag{10}$$

where $0 < \gamma < 1$. This concludes the proof of Lemma 4.2. □

Lemma 4.3. *For each time t, the difference process of $\hat{Q}_t(s_t,c_t)$ and $Q^*(s_t,c_t)$ satisfies the following relations asymptotically with probability one: $\hat{Q}_t(s_t,c_t) - Q^*(s_t,c_t) \le B\bullet n_{\boxtimes} t^{R-1}$ if $R \in (1-\gamma, 1\bullet 2)$ and $\hat{Q}_t(s_t,c_t) - Q^*(s_t,c_t) \le B\sqrt{\log\log n_{\boxtimes} t \bullet n_{\boxtimes} t}$, otherwise, where $B > 0$ is some constant.*

Proof. The proof follows [57, 62] by generalizing the point-based update to the region-based update. Specifically, $n_{\boxtimes}$ is introduced to denote the number of state-configuration pairs in the region for the region-based update, while $n_{\boxtimes} = 1$ for the point-based update. The details are omitted due to the space limitation. □

As t goes to infinity, the difference process of $\hat{Q}_t\ s_t, c_t$ and $Q\ \ s_t, c_t$ converges to zero asymptotically with probability one based on Lemma 4.3. Therefore, the performance gap is determined by Lemma 4.2. The convergence rate can be obtained from Lemma 4.3. This concludes the proof of Theorem 4.1. □

Remarks: Theorem 4.1 confirms our intuition that the RRL approach can accelerate the convergence speed of the reinforcement learning such that the larger $n_{\boxtimes}$ (i.e., the larger δ), the faster the RRL converges. However, the fast convergence speed is at the cost of performance loss, i.e., there would be a gap $\frac{\Delta}{1-\boxtimes}$ between the RRL and the optimal solution. When $\delta = 0$, we have $n_{\boxtimes} = 1$ and $\Delta = 0$, and the results of Theorem 4.1 degenerates to the results for the traditional point-based reinforcement learning [62]. *Thanks to the unique structure of our problem (see Fig. 6), we are able to choose a suitable size of the region such that the convergence speed can be significantly improved with near optimal performance (see Section 6).* Note that the proof of Lemma 4.3 generalizes the proof of [62] by not only using the region-based update but also relaxing the learning rate conditions in [62] by following [57], in order to avoid sub-optimal solutions in the original proof of [62].

5 IMPLEMENTATION

In this section, we discuss how we implement the proposed approach in machine learning serving systems, focusing on the design of neural network based estimation function and the Tensorflow Serving integration of the proposed framework.

5.1 Neural Network based Estimation Function

As discussed in Section 4, it is challenging to characterize the estimation function in a closed form. Neural network based approaches have shown great potentials in many applications [54, 55]. In this paper, we propose a neural network based estimation function. One key challenge is how to find a suitable neural network structure for the estimation function (1) to support swift machine learning serving scheduling. If a simple network structure is used, it may not effectively capture the structure of the underlying state-configuration space, which may lead to high estimation error; if a complicated network structure is used, it may take a long training time, which is not suitable for online serving systems.

To strike a balance between complexity and efficiency, we use an evolutionary algorithm NEAT [58] to guide the design of network structure. The network we designed has two hidden layers (one with 256 neurons and the other with 64 neurons) using ReLu[43] as activation function and one output layer with linear activation, after experimenting different network structures. In this paper, the network parameters are optimized using Follow-the-regularized-Leader (FTRL)[6] optimizer instead of the Adam method or other popular optimizers [33, 72]. This is because the number of training samples in our problem is far less than the number of state-configuration pairs in the space when doing online tuning, and thus FTRL performs very well here. Moreover, FTRL is insensitive to model parameters. Our experiments in Tensorflow Serving show that FTRL performs well even where there is limited training data. (see Section 6).

5.2 Tensor□ow Serving Integration

We integrate the proposed scheduling framework into Tensorflow Serving [44], a popular production-ready machine learning serving system. While we do a case study with Tensorflow serving, nothing prevents the proposed work being integrated with other machine learning serving systems as we do not use anything Tensorflow specific features. In the interest of space, we only briefly highlight our main implementation design.

Pro□ler: Though TensorBoard [2] offers sophisticated visualization and logging capabilities for training machine learning models using Tensorflow, it provides no support for Tensorflow Serving. Therefore, we implement a lightweight profiler that can continuously monitor the workload and track request latency by instrumenting the *DirectSession* and *gRPC* modules and implementing the dispatch queue as discussed next. In this way, the overall execution time is split into waiting time, service time, and network delay. For GPU monitoring, we also use NVIDIA System Management Interface (NVIDIA-SMI) running as daemon to profile real-time GPU performance information such as utilization. We collect request arrival rate, real-time request latency and system resource utilization from Tensorflow Serving. Since our framework is designed to be lightweight and portable, we do not use hardware level integration. Rather we rely on the metrics reported by third party software such as Tensorflow Serving and NVIDIA-SMI. Their reported metrics may have error yet the nature of reinforcement learning and the reward estimation of RRL enables our framework to be error-tolerant, which is validated by the evaluation results in Section 6. The metrics are reported by Profiler in real-time, so it serves as a performance monitor for Scheduler to identify network congestion and single-point failure in the cluster.

Scheduler: Tensorflow Serving does not support request level parallelism, so we implement a flexible dispatch queue that supports plugin scheduling policies (e.g., users can specify scheduling objective such as minimizing latency, achieving SLO while minimizing resources). The dispatch queue follows the scheduling policies from the RRL module and assigns requests to the target node with pre-computed inter-op and intra-op parallelism. Current implementation of Tensorflow serving sets inter-op according to intra-op parallelism. Thus we modify *ModelServer* to enable fine grained control of inter-op and intra-op parallelism. The Scheduler is failure-aware to reduce the risk of breaking SLO due to node failures.

RRL: We implement the RRL as a module that takes inputs of the monitoring information from Profiler to compute and update scheduling policies and feed to the Scheduler. The RRL module allows asynchronous neural network training to put little extra overhead to the serving system. The neural network is trained with all previous seen samples until hitting either the training step or training loss threshold.

6 EXPERIMENTAL EVALUATION

In this section, we conduct extensive experimental evaluation to verify the effectiveness and robustness of the proposed RRL-based scheduling framework using a rich selection of state-of-the-art machine learning applications on both CPU and GPU based infrastructure. We first evaluate the sensitivity of RRL in convergence speed by adjusting the region size. Then we compare RRL with the

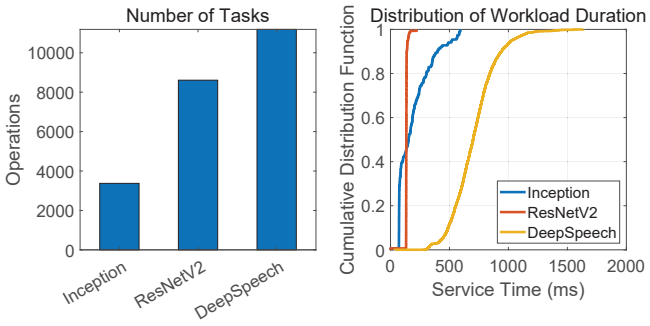

Figure 10: The number of tasks and the distribution of request duration of service workloads measured on CPU infrastructure.

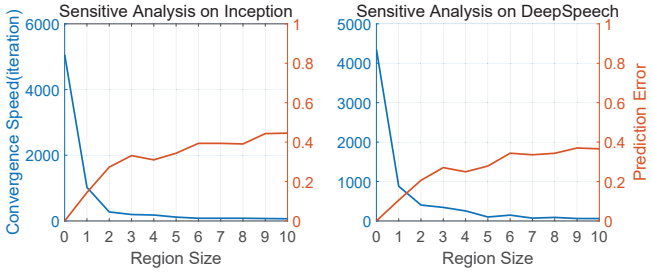

Figure 11: Sensitivity analysis of RRL in terms of the convergence time in iteration (left y-axis) and the prediction error (right y-axis) as a function of region size using Inception and DeepSpeech.

latest reinforcement learning approaches in the following aspects: (i) effectiveness in terms of minimizing latency; (ii) robustness in dynamic workload; (iii) strict SLO guarantee; (iv) effectiveness of meeting SLO while minimizing resource usage.

6.1 Experimental Setup

Machine Learning Serving System: We prototype RRL based scheduling framework and integrate it in Tensorflow Serving, refer to Section 5.2 for more details.

Service Workloads: We use three popular machine learning applications for evaluation:

Inception V3 [61]: popular deep convolutional neural network based image classification model classifies 256x256 color images in 1,000 categories with 48 layers and tens of millions parameters. Serving requests are from ImageNet 22K dataset [52] with homogeneous sizes.

Inception ResNet V2 [60]: advanced deep convolutional neural network based image classification model with the aid of ResNet[26] that allows network with depth of 162 layers and hundreds of millions of parameters. Serving requests are from ImageNet 22K dataset [52] with homogeneous sizes.

Deep Speech V2 [8]: popular deep recurrent neural network based speech to text model with 11 layers. Serving requests samples are from TeD talk dataset [51] and with heterogeneous sizes.

Inception, ResNet, and Deepspeech are representative models for Convolutional Neural Networks, Residual Neural Network, and Recurrent Neural Network, covering popular ML-serving application domains such as computer vision and natural language processing. The number of tasks and the request duration of servive workloads are illustrated in Fig. 10, where the request duration of Inception and ResNet are homogeneous while Deepspeech is heterogenous.

Arrival Process: We use two non-exponential arrival processes for evaluation:

WiKi: given there is no public available ML serving trace, we opt for traces of user traffic visiting Wikipedia website [66] with unpredictable load spikes.

Dynamic: a synthetic dynamic arrival process composed of periods of Poison process with randomly changing average, which has more pronounced changes from one period to the next.

Hardware: We use a cluster of 10 identical servers. Each of them is equipped with dual-sockets Intel(R) Xeon(R) CPU E5-2630 v4 @ 2.20GHz and four NVIDIA GeForce GTX 1080 Ti GPUs, 64 GB of memory, and connected through Infiniband. One sever is acting as client, one server is used as dispatch queue, and the rest are request processing severs.

Baseline Approaches: Since there is no alternative intelligent scheduling framework for a direct comparison, we opt to implement the state-of-the-art reinforcement learning approaches for tuning parallelism configuration in our scheduling framework: DeepRM [38] and CAPES [37], as they are the closest approaches for online ML-serving scheduling. CAPES is a general-purpose parameter tuning algorithm and DeepRM is a job scheduling algorithm designed to work under limited resources. Both DeepRM and CAPES are open-sourced, so we use their codes published at github and set parameters according their papers [37, 38]. Specifically, in the structure level, DeepRM uses one hidden layer of 20 neurons and CAPES uses 2 hidden layers of 200 neurons. Both of them are trained with RMSProp [65] with the learning rate of 0.001 according to their original design. For fair comparison, we feed the profiling metrics (e.g., latency and resource utilization) provided by Profiler into the reward function and use both the profiling metrics and rewards as the input parameters of DeepRM and CAPES to compute the corresponding output parameters, which are interpreted by the Scheduler afterwards. We assign a dedicated server to do the reinforcement learning tasks so that the learning tasks are not interfered with the inference tasks. Our evaluation results suggest that our deployment of both DeepRM and CAPES is consistent with their paper and could identify reasonably good configurations, see Fig. 12.

SLO setting: As our testbed is not production level, we set relatively loose SLOs in our evaluation, i.e., a range between 1800ms and 3200ms to emulate different latency requirements for ML serving in production environments, which is consistent with previous studies [69, 70, 74].

6.2 Convergence Speed Analysis of RRL

The key tuning parameter in RRL is the region size as it controls the trade-off between convergence speed and accuracy. We perform sensitivity analysis of RRL to verify the theoretical results

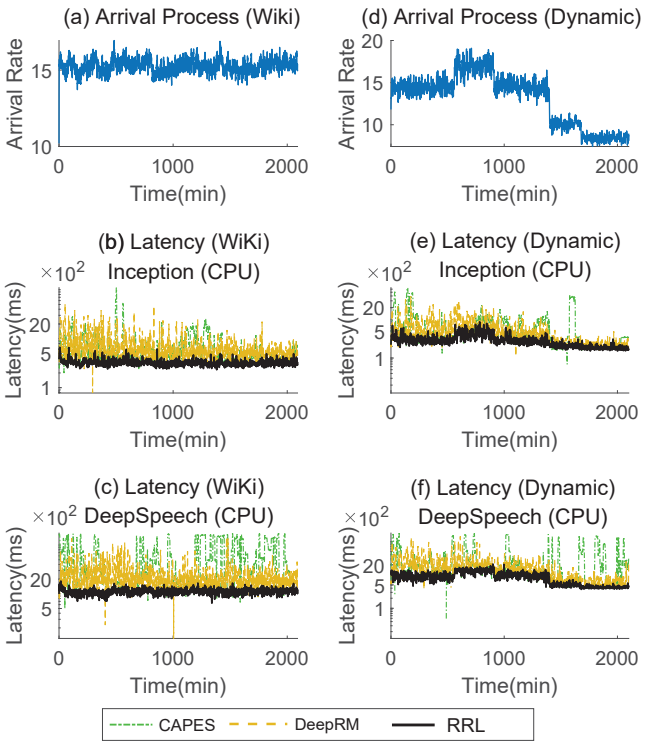

Figure 12: Comparisons of RRL with CAPES and DeepRM under different arrival processes and service workloads. The first column (a)(b)(c) shows the first scheduling objective of minimizing latency using WiKi as arrival process for Inception and DeepSpeech; the second column (d)(e)(f) also shows the scheduling objective of minimizing latency but under dynamic arrival process for Inception and DeepSpeech.

in Theorem 4.1 using Inception, as illustrated in Fig. 11. The results show the convergence time measured in iteration (left y-axis) and distance from optimal Q-learning function (right y-axis) as a function of the region size. It is clear that convergence time drops very quickly when the region size increases while the accuracy moves away from optimal in a much slower speed. For example, when the region size is one, RRL converges five times faster than Q-learning, which verifies the potential of the region based methodology. When region size is zero, RRL degenerates to point-based learning, which has the same accuracy and the longest convergence time as Q learning. The region size can be adjusted according to user's performance and convergence time needs. The experimental results show that RRL converge to near optimal performance 8 times faster than state-of-the-art approaches DeepRM[38] and CAPES[37].

6.3 E□ ectiveness of Minimizing Serving Latency

In this section, we compare the effectiveness of minimizing serving latency between RRL and the two baseline Deep Reinforcement Learning approaches: DeepRM[38] and CAPES[37] on both CPU and GPU based infrastructure. It is worth noting that given our testbed is not enterprise scale nor equipped with latest hardware,

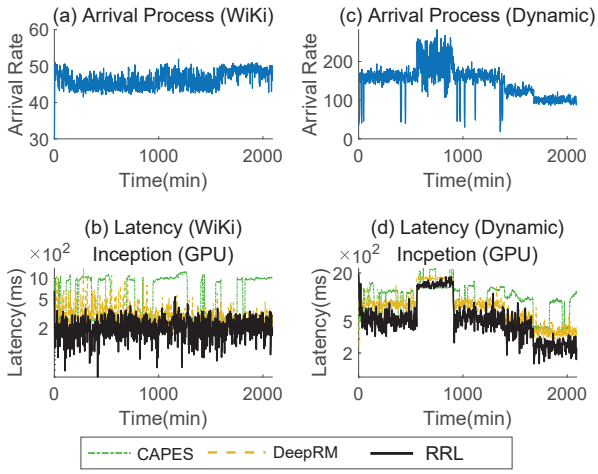

Figure 13: Comparisons of RRL with CAPES and DeepRM under different arrival processes and service workloads. The first column (a)(b)(c) shows the first scheduling objective of minimizing latency using WiKi as arrival process for Inception on GPU; the second column (d)(e)(f) also shows the scheduling objective of minimizing latency but under dynamic arrival process for Inception on GPU.

the latency is relatively high due to high queuing waiting time. However, the purpose here is to show the relative performance comparison between different scheduling methods rather than achieving record-breaking performance measure.

CPU Cluster. We show latency results of Inception and DeepSpeech running on CPU cluster in Fig. 12(b) and Fig. 12(c), respectively. Both experiments use WiKi trace to drive the arrival process, which is demonstrated in Fig. 12(a). The WiKi workload demonstrates random traffic pattern with a relatively steady average inter-arrival rate over time. The results verify that RRL converges much faster than the baseline approaches, i.e., RRL converges to a near optimal performance in less than 200 minutes, while DeepRM roughly converges around 1700 minutes with variance and CAPES could not converge even after 2000 minutes. The results also show that RRL is able to achieve better latency performance compared to deep reinforcement learning based approaches, thanks to the swift learning capabilities. More specifically, the average latency of RRL improves from CAPES by 79.0% and DeepRM by 51.7% for DeepSpeech and improves from CAPES and DeepRM by 50.6% and 52.9% respectively for Inception.

GPU Cluster. As explained in earlier sections, the parallelism on GPU is controlled by the hardware scheduler and difficult to be adjusted through software approaches. Here we control the parallelism using an indirect approach by tuning the batching parameters (parallel batch threads, batch size, and batch timeout). Similar as CPU case, we use WiKi workload and CAPES and DeepRM as baselines and report the results in Fig. 13. It is clear that the variance in latency is higher compared to the CPU results, which is caused by the indirect control mechanism as the interaction between batching and hardware scheduler is more complex. Despite of the challenge of more complex interactions, RRL still converges quickly and outperforms CAPES and DeepRM in latency. Specifically, RRL performs 30.3% better than DeepRM and 47.1% than CAPES.

6.4 Robustness under Dynamic Workload

Workload can change dynamically over time in practice, so it is important to have swift adaptivity. In this section, we evaluate the robustness of the proposed scheduling framework in terms of the ability to quickly adapt to the workload change. We use a synthetic dynamic arrival process for evaluation, as shown in Fig. 12(d), the arrival change is more pronounced than the WiKi arrival process, which emulates the change of user traffic patterns over time.

CPU Cluster. The latency results on CPU cluster for Inception and DeepSpeech are shown in Fig. 12(e) and Fig. 12(f), respectively. The results suggest that RRL can adapt to the user traffic change very quickly. Thanks to the region-based learning approach, the number of samples that RRL needs for updating scheduling policy is far less than point-based approaches, which leads to a much shorter adapting time compared to CAPES and DeepRM. The latency results also show that RRL has a more stable latency performance compared to deep reinforcement learning based approaches. In contrast, DeepRM takes a much longer time to update scheduling polices and CAPES shows significant variation due to its slow learning process. On average, RRL reduces the latency of DeepSpeech by 69.3% and 49.2% compared to CAPES and DeepRM respectively, and 58.1% and 45.8% for Inception respectively.

GPU Cluster. We also evaluate the dynamic workload on GPU-based infrastructure. Due to the complex interactions, a side effect brought by indirect control, the adapt speed is slower than CPU case. However, even in this challenging scenario, RRL still consistently outperforms CAPES and DeepRM by 38.0% and 69.1% on average respectively.

6.5 Meeting Strict SLO

We evaluate our approach under the scenario of meeting strict SLO target, i.e., 95th percentile latency SLO of 550ms for CPU and 520ms for GPU. [4] Fig. 14 (note the logscale in both axes) demonstrates that the CCDF latency comparison of RRL with CAPES and DeepRM using CPU cluster and GPU cluster, respectively. Overall, RRL achieves a much shorter tail latency compared to CAPES and DeepRM. From the tail comparison, it is clear that RRL can provide strict SLO guarantee and achieve up to 49.9% SLO violation reduction compared to CAPES and up to 43.4% compared to DeepRM, thanks to its SLO-aware design.

6.6 Meeting SLO With Minimum Resources

Another common scheduling objective is meeting relatively loose SLO while minimizing the resource usage (e.g., cloud environment or shared cluster), which is also supported by our scheduling framework. Fig. 15 provide a case study of this scheduling objective using DeepSpeech, ResNet, and Inception under dynamic workload on CPU and GPU infrastructure, respectively.

CPU Cluster. The latency of DeepSpeech over the time running on CPU cluster using different scheduling methods is present in Fig. 15(b), where both CAPES and DeepRM perform poorly on achieving the SLO target. CAPES spent around 200 minutes before finding a scheduling policy that can achieve the SLO but at the expense of high CPU utilization whereas DeepRM violates the SLO whenever the workload has significant changes. RRL on the contrast always guarantees the SLO, even during abrupt workload changes. Another comparison is on resource utilization, which is very important for consolidating resources and achieve cost efficient serving. We report the CPU utilization at Fig. 15(c), where RRL consistently consumes much less CPU resource than both CAPES and DeepRM and provides great potential for workload consolidation and/or cost saving, which is especially important for serving machine learning models in cloud environment. Similar observations holds for the ResNet results in Fig. 15(e)(f), where all three methods achieve SLO in a short time, but RRL uses only one fourth CPU resources compared to the deep reinforcement learning abased methods. On average, the average CPU resources saved by RRL for DeepSpeech is 13.4% compared to CAPES and 8.5% compared to DeepRM. For ResNet, the resource saving is even more significant: RRL on average saved 52.9% from CAPES and 46.8% from DeepRM.

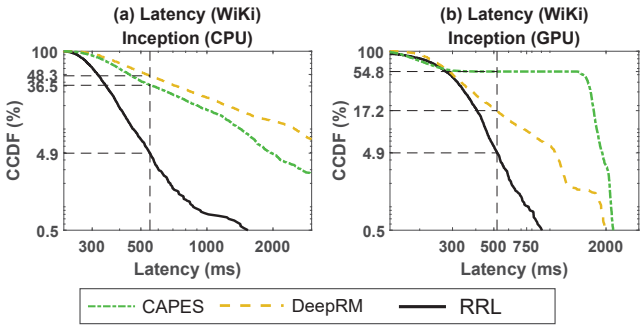

Figure 14: Comparisons of RRL with CAPES and DeepRM under strict SLO (95th percentile latency of 550ms for CPU and 520ms for GPU).

GPU Cluster. We show the GPU results in Fig. 15(h)(i), where RRL keeps a stable latency right under SLO and only uses half GPU resources compared with CAPES and DeepRM. On average, RRL saved 10.6% GPU resources compared with CAPES and 12.9% GPU resources from DeepRM. Considering the high cost of GPU, such saving is not trivial.

6.7 Discussion

Evaluation results show that RRL outperforms the standard deep reinforcement learning methods in both speed and accuracy, in spite of the estimation error in RRL, when environment/workload changes quickly. RRL uses the unique characteristics of ML-serving to accelerate the learning process: when parallelism changes, the latency is quite versatile globally while smooth locally. Other methods do not have such insights. When environment/workload changes, RRL may have already converged to a near optimal solution, whereas other methods may be still far away. Therefore, in online systems, RRL outperforms the standard deep reinforcement learning methods in both speed and accuracy.

7 CONCLUSION AND FUTURE WORK

In this paper, we proposed a RRL-based scheduling framework for machine learning serving that can efficiently identify the optimal

[4] It is worth to emphasize again that the relative high latency is because our testbed is not enterprise scale nor equipped with latest hardware, so both the processing time and the queuing waiting time is relatively high.

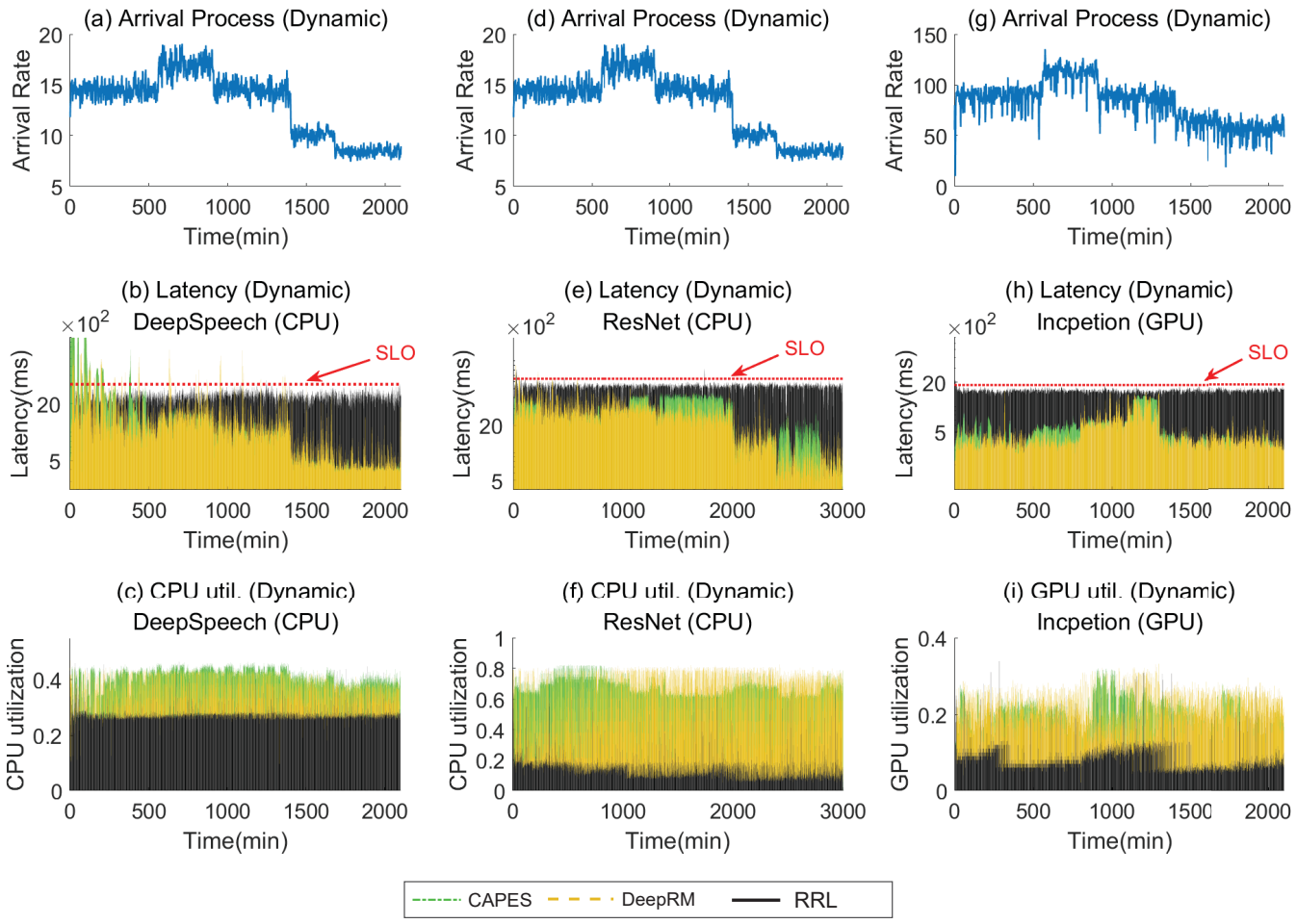

Figure 15: Comparisons of RRL with CAPES and DeepRM when achieving SLO while optimizing resource usage (i.e., CPU and GPU utilization) under dynamic arrival processes and service workloads. (a)-(f) shows the scheduling objective of minimizing CPU utilization with respect to given SLOs for model DeepSpeech and ResNet under dynamic workloads. (g)(h)(i) shows the second scheduling objective of achieving SLO while minimizing GPU usage with Inception under dynamic arrival process. The SLOs for DeepSpeech, ResNet and Inception are 2400ms, 3200ms, and 1850ms, respectively.

configuration under dynamic workloads. A key observation is that the system performance under similar configurations in a region can be accurately estimated by using the system performance under one of these configurations, due to their correlation, based on which we developed the RRL approach. We theoretically showed that the RRL approach can achieve a near optimal solution with fast convergence speed. The proposed framework is prototyped and evaluated on Tensorflow serving system and can be easily extended to other machine learning serving systems. Extensive experimental evaluation on both CPU cluster and GPU cluster show that RRL can quickly adapt to the dynamics of workloads and system environments. Compared to the state-of-the-art Deep Reinforcement Learning based methods (DeepRM and CAPES), the proposed scheduling framework can reduce the average latency by up to 79.0% on CPU cluster and 69.3% on GPU cluster. In the SLO-aware scenario, RRL reduces up to 49.9% SLO violation under strict SLO requirement while reducing the resource usage by up to 52.9% on CPU and 12.9% on GPU in loose SLO scenario. In addition, the proposed solution does not have assumptions on workload or underlying systems and thus can be used for most modern machine learning systems and applications.

ACKNOWLEDGMENT

This work is supported in part by the following grants: National Science Foundation CCF-1756013, IIS-1838024 (using resources provided by Amazon Web Services as part of the NSF BIGDATA program), EEC-1801727, and Amazon Web Services Cloud Credits for Research Award. We also acknowledge the support of Research & Innovation and the Office of Information Technology at the University of Nevada, Reno for computing time on the Pronghorn High-Performance Computing Cluster. We thank the anonymous reviewers for their insightful comments and suggestions.

REFERENCES

[1] 2019. Intel(R) Math Kernel Library for Deep Neural Networks (Intel(R) MKL-DNN). https://github.com/intel/mkl-dnn

[2] 2019. TensorBoard: TensorFlow's Visualization Toolkit. https://github.com/tensorflow/tensorboard

[3] 2019. TensorFlow XLA. https://www.tensorflow.org/performance/xla/

[4] Emile Aarts and Jan Korst. 1988. Simulated annealing and Boltzmann machines. (1988).

[5] Martín Abadi, Ashish Agarwal, Paul Barham, Eugene Brevdo, Zhifeng Chen, Craig Citro, Gregory S. Corrado, Andy Davis, Jeffrey Dean, Matthieu Devin, Sanjay Ghemawat, Ian J. Goodfellow, Andrew Harp, Geoffrey Irving, Michael Isard, Yangqing Jia, Rafal Józefowicz, Lukasz Kaiser, Manjunath Kudlur, Josh Levenberg, Dan Mané, Rajat Monga, Sherry Moore, Derek Gordon Murray, Chris Olah, Mike Schuster, Jonathon Shlens, Benoit Steiner, Ilya Sutskever, Kunal Talwar, Paul A. Tucker, Vincent Vanhoucke, Vijay Vasudevan, Fernanda B. Viégas, Oriol Vinyals, Pete Warden, Martin Wattenberg, Martin Wicke, Yuan Yu, and Xiaoqiang Zheng. 2016. TensorFlow: Large-Scale Machine Learning on Heterogeneous Distributed Systems. *CoRR* abs/1603.04467 (2016). arXiv:1603.04467 http://arxiv.org/abs/1603.04467

[6] Jacob D Abernethy, Elad Hazan, and Alexander Rakhlin. 2009. Competing in the dark: An efficient algorithm for bandit linear optimization. (2009).

[7] Omid Alipourfard, Hongqiang Harry Liu, Jianshu Chen, Shivaram Venkataraman, Minlan Yu, and Ming Zhang. 2017. CherryPick: Adaptively Unearthing the Best Cloud Configurations for Big Data Analytics.. In *NSDI*, Vol. 2. 4–2.

[8] Dario Amodei, Sundaram Ananthanarayanan, Rishita Anubhai, Jingliang Bai, Eric Battenberg, Carl Case, Jared Casper, Bryan Catanzaro, Qiang Cheng, Guoliang Chen, et al. 2016. Deep speech 2: End-to-end speech recognition in english and mandarin. In *International Conference on Machine Learning*. 173–182.

[9] Jacob Andreas, Marcus Rohrbach, Trevor Darrell, and Dan Klein. 2016. Learning to Compose Neural Networks for Question Answering. *CoRR* abs/1601.01705 (2016). arXiv:1601.01705 http://arxiv.org/abs/1601.01705

[10] AWSLABS. 2019. Mxnet model server. https://github.com/awslabs/mxnet-model-server.

[11] Mohammad Gheshlaghi Azar, Remi Munos, Mohammad Ghavamzadeh, and Hilbert Kappen. 2011. Speedy Q-learning. In *Advances in neural information processing systems*.

[12] Muthu Manikandan Baskaran, Uday Bondhugula, Sriram Krishnamoorthy, J. Ramanujam, Atanas Rountev, and P. Sadayappan. 2008. A Compiler Framework for Optimization of Affine Loop Nests for Gpgpus. In *Proceedings of the 22Nd Annual International Conference on Supercomputing (ICS '08)*. ACM, New York, NY, USA, 225–234.

[13] Léon Bottou. 2010. Large-scale machine learning with stochastic gradient descent. In *COMPSTAT*.

[14] Tianshi Chen, Zidong Du, Ninghui Sun, Jia Wang, Chengyong Wu, Yunji Chen, and Olivier Temam. 2014. DianNao: A Small-footprint High-throughput Accelerator for Ubiquitous Machine-learning. In *ASPLOS*.

[15] Dazhao Cheng, Yuan Chen, Xiaobo Zhou, Daniel Gmach, and Dejan Milojicic. 2017. Adaptive scheduling of parallel jobs in spark streaming. In *INFOCOM 2017-IEEE Conference on Computer Communications, IEEE*. IEEE, 1–9.

[16] Heng-Tze Cheng, Levent Koc, Jeremiah Harmsen, Tal Shaked, Tushar Chandra, Hrishi Aradhye, Glen Anderson, Greg Corrado, Wei Chai, Mustafa Ispir, et al. 2016. Wide & deep learning for recommender systems. In *Proceedings of the 1st Workshop on Deep Learning for Recommender Systems*. ACM, 7–10.

[17] Trishul Chilimbi, Johnson Apacible, Karthik Kalyanaraman, and Yutaka Suzue. 2014. Project Adam: Building an Efficient and Scalable Deep Learning Training System. In *OSDI*.

[18] Daniel Crankshaw, Xin Wang, Giulio Zhou, Michael J. Franklin, Joseph E. Gonzalez, and Ion Stoica. 2017. Clipper: A Low-Latency Online Prediction Serving System. In *14th USENIX Symposium on Networked Systems Design and Implementation, NSDI 2017, Boston, MA, USA, March 27-29, 2017*. 613–627.

[19] G. E. Dahl, Dong Yu, Li Deng, and A. Acero. 2012. Context-Dependent Pre-Trained Deep Neural Networks for Large-Vocabulary Speech Recognition. *TASLP* (2012).

[20] Jeffrey Dean, Greg Corrado, Rajat Monga, Kai Chen, Matthieu Devin, Quoc V. Le, Mark Z. Mao, Marc'Aurelio Ranzato, Andrew W. Senior, Paul A. Tucker, Ke Yang, and Andrew Y. Ng. 2012. Large Scale Distributed Deep Networks.. In *NIPS*.

[21] Adithya M Devraj and Sean P Meyn. 2017. Fastest Convergence for Q-learning. *arXiv preprint arXiv:1707.03770* (2017).

[22] Thomas G Dietterich and Nicholas S Flann. 1997. Explanation-based learning and reinforcement learning: A unified view. *Machine Learning* 28, 2-3 (1997), 169–210.

[23] Arpan Gujarati, Sameh Elnikety, Yuxiong He, Kathryn S. McKinley, and Björn B. Brandenburg. 2017. Swayam: distributed autoscaling to meet SLAs of machine learning inference services with resource efficiency. In *Proceedings of the 18th ACM/IFIP/USENIX Middleware Conference, Las Vegas, NV, USA, December 11 - 15, 2017*, K. R. Jayaram, Anshul Gandhi, Bettina Kemme, and Peter R. Pietzuch (Eds.). ACM, 109–120.

[24] Awni Y. Hannun, Carl Case, Jared Casper, Bryan Catanzaro, Greg Diamos, Erich Elsen, Ryan Prenger, Sanjeev Satheesh, Shubho Sengupta, Adam Coates, and Andrew Y. Ng. 2014. Deep Speech: Scaling up end-to-end speech recognition. *CoRR* abs/1412.5567 (2014). arXiv:1412.5567 http://arxiv.org/abs/1412.5567

[25] Md. E. Haque, Yong Hun Eom, Yuxiong He, Sameh Elnikety, Ricardo Bianchini, and Kathryn S. McKinley. 2015. Few-to-Many: Incremental Parallelism for Reducing Tail Latency in Interactive Services. In *ASPLOS*.

[26] Kaiming He, Xiangyu Zhang, Shaoqing Ren, and Jian Sun. 2016. Deep residual learning for image recognition. In *Proceedings of the IEEE conference on computer vision and pattern recognition*. 770–778.

[27] Forrest N Iandola, Song Han, Matthew W Moskewicz, Khalid Ashraf, William J Dally, and Kurt Keutzer. 2016. Squeezenet: Alexnet-level accuracy with 50x fewer parameters and< 0.5 mb model size. *arXiv preprint arXiv:1602.07360* (2016).

[28] Google Inc. 2019. Google Cloud Vision API. https://cloud.google.com/vision/.

[29] Florin Isaila, Guido Malpohl, Vlad Olaru, Gabor Szeder, and Walter Tichy. 2004. Integrating Collective I/O and Cooperative Caching into the "Clusterfile" Parallel File System. In *Proceedings of the 18th Annual International Conference on Supercomputing (ICS '04)*. ACM, New York, NY, USA, 58–67.

[30] Myeongjae Jeon, Yuxiong He, Sameh Elnikety, Alan L. Cox, and Scott Rixner. 2013. Adaptive Parallelism for Web Search. In *EuroSys*.

[31] Myeongjae Jeon, Yuxiong He, Sameh Elnikety, Alan L Cox, and Scott Rixner. 2013. Adaptive parallelism for web search. In *Proceedings of the 8th ACM European Conference on Computer Systems*. ACM, 155–168.

[32] Hamzeh Khazaei, Jelena V. Misic, and Vojislav B. Misic. 2012. Performance Analysis of Cloud Computing Centers Using M/G/m/m+r Queuing Systems. *IEEE Trans. Parallel Distrib. Syst.* 23, 5 (2012), 936–943.

[33] Diederik P. Kingma and Jimmy Ba. 2015. Adam: A Method for Stochastic Optimization. In *3rd International Conference on Learning Representations, ICLR 2015, San Diego, CA, USA, May 7-9, 2015, Conference Track Proceedings*, Yoshua Bengio and Yann LeCun (Eds.). http://arxiv.org/abs/1412.6980

[34] Sriram Krishnamoorthy, Ümit V. Çatalyürek, Jarek Nieplocha, Atanas Rountev, and P. Sadayappan. 2006. Data management and query - Hypergraph partitioning for automatic memory hierarchy management. In *Proceedings of the ACM/IEEE SC2006 Conference on High Performance Networking and Computing, November 11-17, 2006, Tampa, FL, USA*. ACM Press, 98.

[35] Alex Krizhevsky, Ilya Sutskever, and Geoffrey E. Hinton. 2017. ImageNet classification with deep convolutional neural networks. *Commun. ACM* 60, 6 (2017), 84–90.

[36] Min Li, Liangzhao Zeng, Shicong Meng, Jian Tan, Li Zhang, Ali R Butt, and Nicholas Fuller. 2014. Mronline: Mapreduce online performance tuning. In *Proceedings of the 23rd international symposium on High-performance parallel and distributed computing*. ACM, 165–176.

[37] Yan Li, Kenneth Chang, Oceane Bel, Ethan L Miller, and Darrell DE Long. 2017. CAPES: unsupervised storage performance tuning using neural network-based deep reinforcement learning. In *Proceedings of the International Conference for High Performance Computing, Networking, Storage and Analysis*. ACM, 42.

[38] Hongzi Mao, Mohammad Alizadeh, Ishai Menache, and Srikanth Kandula. 2016. Resource management with deep reinforcement learning. In *Proceedings of the 15th ACM Workshop on Hot Topics in Networks*. ACM, 50–56.

[39] Robert Mcmillan. 2019. How Skype Used AI to Build Its Amazing New Language Translator. http://www.wired.com/2014/12/skype-used-ai-build-amazing-new-language-translator/.

[40] Cataldo Mega, Tim Waizenegger, David Lebutsch, Stefan Schleipen, and JM Barney. 2014. Dynamic cloud service topology adaption for minimizing resources while meeting performance goals. *IBM Journal of Research and Development* 58, 2/3 (2014), 8–1.

[41] Azalia Mirhoseini, Hieu Pham, Quoc V Le, Benoit Steiner, Rasmus Larsen, Yuefeng Zhou, Naveen Kumar, Mohammad Norouzi, Samy Bengio, and Jeff Dean. 2017. Device placement optimization with reinforcement learning. *arXiv preprint arXiv:1706.04972* (2017).

[42] Fiona Fui-Hoon Nah. 2003. A Study on Tolerable Waiting Time: How Long Are Web Users Willing to Wait?. In *9th Americas Conference on Information Systems, AMCIS 2003, Tampa, FL, USA, August 4-6, 2003*. Association for Information Systems, 285. http://aisel.aisnet.org/amcis2003/285

[43] Vinod Nair and Geoffrey E Hinton. 2010. Rectified linear units improve restricted boltzmann machines. In *Proceedings of the 27th international conference on machine learning (ICML-10)*. 807–814.

[44] Christopher Olston, Noah Fiedel, Kiril Gorovoy, Jeremiah Harmsen, Li Lao, Fangwei Li, Vinu Rajashekhar, Sukriti Ramesh, and Jordan Soyke. 2017. TensorFlow-Serving: Flexible, High-Performance ML Serving. *arXiv preprint arXiv:1712.06139* (2017).

[45] James Oly and Daniel A. Reed. 2002. Markov model prediction of I/O requests for scientific applications. In *Proceedings of the 16th international conference on Supercomputing, ICS 2002, New York City, NY, USA, June 22-26, 2002*, Kemal Ebcioglu, Keshav Pingali, and Alex Nicolau (Eds.). ACM, 147–155.

[46] Kalin Ovtcharov, Olatunji Ruwase, Joo-Young Kim, Jeremy Fowers, Karin Strauss, and Eric S. Chung. 2015. Accelerating Deep Convolutional Neural Networks Using Specialized Hardware. http://research.microsoft.com/apps/pubs/default.

aspx?id=240715

[47] Arun Raman, Hanjun Kim, Taewook Oh, Jae W. Lee, and David I. August. 2011. Parallelism orchestration using DoPE: the degree of parallelism executive. In *Proceedings of the 32nd ACM SIGPLAN Conference on Programming Language Design and Implementation, PLDI 2011, San Jose, CA, USA, June 4-8, 2011*. 26–37.

[48] Bharath Ramsundar, Steven Kearnes, Patrick Riley, Dale Webster, David Konerding, and Vijay Pande. 2015. Massively Multitask Networks for Drug Discovery. *arXiv preprint arXiv:1502.02072* (2015).

[49] Mauro Ribeiro, Katarina Grolinger, and Miriam AM Capretz. 2015. Mlaas: Machine learning as a service. In *2015 IEEE 14th International Conference on Machine Learning and Applications (ICMLA)*. IEEE, 896–902.

[50] Chuck Rosenberg. 2019. Improving Photo Search: A Step Across the Semantic Gap. http://googleresearch.blogspot.com/2013/06/improving-photo-search-step-across.html.

[51] Anthony Rousseau, Paul Deléglise, and Yannick Esteve. 2014. Enhancing the TED-LIUM Corpus with Selected Data for Language Modeling and More TED Talks.. In *LREC*. 3935–3939.

[52] Olga Russakovsky, Jia Deng, Hao Su, Jonathan Krause, Sanjeev Satheesh, Sean Ma, Zhiheng Huang, Andrej Karpathy, Aditya Khosla, Michael Bernstein, Alexander C. Berg, and Li Fei-Fei. 2015. ImageNet Large Scale Visual Recognition Challenge. *International Journal of Computer Vision (IJCV)* 115, 3 (2015), 211–252.

[53] Hitoshi Sakagami, Hitoshi Murai, Yoshiki Seo, and Mitsuo Yokokawa. 2002. 14.9 TFLOPS three-dimensional fluid simulation for fusion science with HPF on the Earth Simulator. In *Proceedings of the 2002 ACM/IEEE conference on Supercomputing, Baltimore, Maryland, USA, November 16-22, 2002, CD-ROM*, Roscoe C. Giles, Daniel A. Reed, and Kathryn Kelley (Eds.). IEEE Computer Society, 21:1–21:14. http://ieeexplore.ieee.org/xpl/mostRecentIssue.jsp?punumber=10618

[54] John Schulman, Philipp Moritz, Sergey Levine, Michael Jordan, and Pieter Abbeel. 2015. High-dimensional continuous control using generalized advantage estimation. *arXiv preprint arXiv:1506.02438* (2015).

[55] David Silver, Aja Huang, Chris J Maddison, Arthur Guez, Laurent Sifre, George Van Den Driessche, Julian Schrittwieser, Ioannis Antonoglou, Veda Panneershelvam, Marc Lanctot, et al. 2016. Mastering the game of Go with deep neural networks and tree search. *nature* 529, 7587 (2016), 484.

[56] Satinder P Singh, Tommi Jaakkola, and Michael I Jordan. 1995. Reinforcement learning with soft state aggregation. In *Advances in neural information processing systems*. 361–368.

[57] Satinder P. Singh, Tommi S. Jaakkola, Michael L. Littman, and Csaba Szepesvári. 2000. Convergence Results for Single-Step On-Policy Reinforcement-Learning Algorithms. *Machine Learning* 38, 3 (2000), 287–308.

[58] Kenneth O. Stanley and Risto Miikkulainen. 2002. Evolving Neural Network through Augmenting Topologies. *Evolutionary Computation* 10, 2 (2002), 99–127.

[59] Richard S Sutton, David A McAllester, Satinder P Singh, and Yishay Mansour. 2000. Policy gradient methods for reinforcement learning with function approximation. In *Advances in neural information processing systems*. 1057–1063.

[60] Christian Szegedy, Sergey Ioffe, Vincent Vanhoucke, and Alexander A Alemi. 2017. Inception-v4, inception-resnet and the impact of residual connections on learning.. In *AAAI*, Vol. 4. 12.

[61] Christian Szegedy, Vincent Vanhoucke, Sergey Ioffe, Jon Shlens, and Zbigniew Wojna. 2016. Rethinking the inception architecture for computer vision. In *Proceedings of the IEEE conference on computer vision and pattern recognition*. 2818–2826.

[62] Csaba Szepesvári. 1998. The asymptotic convergence-rate of Q-learning. In *Advances in Neural Information Processing Systems*. 1064–1070.

[63] Ying Tan, Wei Liu, and Qinru Qiu. 2009. Adaptive power management using reinforcement learning. In *Proceedings of the 2009 International Conference on Computer-Aided Design*. ACM, 461–467.

[64] Ivan Tanasic, Isaac Gelado, Javier Cabezas, Alex Ramírez, Nacho Navarro, and Mateo Valero. 2014. Enabling preemptive multiprogramming on GPUs. In *ACM/IEEE 41st International Symposium on Computer Architecture, ISCA 2014, Minneapolis, MN, USA, June 14-18, 2014*. IEEE Computer Society, 193–204. http://ieeexplore.ieee.org/xpl/mostRecentIssue.jsp?punumber=6847316

[65] Tijmen Tieleman and Geoffrey Hinton. 2012. Lecture 6.5-rmsprop: Divide the gradient by a running average of its recent magnitude. *COURSERA: Neural networks for machine learning* 4, 2 (2012), 26–31.

[66] Guido Urdaneta, Guillaume Pierre, and Maarten van Steen. 2009. Wikipedia Workload Analysis for Decentralized Hosting. *Elsevier Computer Networks* 53, 11 (July 2009), 1830–1845. http://www.globule.org/publi/WWADH_comnet2009.html.

[67] Oriol Vinyals, Alexander Toshev, Samy Bengio, and Dumitru Erhan. 2019. A picture is worth a thousand (coherent) words: building a natural description of images. http://googleresearch.blogspot.com/2014/11/a-picture-is-worth-thousand-coherent.html.

[68] Christopher JCH Watkins and Peter Dayan. 1992. Q-learning. *Machine learning* 8, 3-4 (1992), 279–292.

[69] Feng Yan, Yuxiong He, Olatunji Ruwase, and Evgenia Smirni. 2016. SERF: efficient scheduling for fast deep neural network serving via judicious parallelism. In *Proceedings of the International Conference for High Performance Computing, Networking, Storage and Analysis, SC 2016, Salt Lake City, UT, USA, November 13-18, 2016*. 300–311.

[70] Feng Yan, Yuxiong He, Olatunji Ruwase, and Evgenia Smirni. 2018. Efficient Deep Neural Network Serving: Fast and Furious. *IEEE Trans. Network and Service Management* 15, 1 (2018), 112–126.

[71] Richard M Yoo, Han Lee, Kingsum Chow, and S Lee Hsien-hsin. 2006. Constructing a non-linear model with neural networks for workload characterization. In *Workload Characterization, 2006 IEEE International Symposium on*. IEEE, 150–159.

[72] Matthew D Zeiler. 2012. ADADELTA: an adaptive learning rate method. *arXiv preprint arXiv:1212.5701* (2012).

[73] Chengliang Zhang, Huangshi Tian, Wei Wang, and Feng Yan. 2018. Stay Fresh: Speculative Synchronization for Fast Distributed Machine Learning. In *The 38th IEEE International Conference on Distributed Computing Systems (ICDCS), Vienna, Austria, July, 2018*.

[74] Chengliang Zhang, Minchen Yu, Wei Wang, and Feng Yan. 2019. MArk: Exploiting Cloud Services for Cost-Effective, SLO-Aware Machine Learning Inference Serving. In *2019 USENIX Annual Technical Conference (USENIX ATC 19)*.

[75] Minjia Zhang, Samyam Rajbhandari, Wenhan Wang, and Yuxiong He. 2018. DeepCPU: Serving RNN-based Deep Learning Models 10x Faster. In *2018 USENIX Annual Technical Conference, USENIX ATC 2018, Boston, MA, USA, July 11-13, 2018*. 951–965.

[76] Minjia Zhang, Samyam Rajbhandari, Wenhan Wang, Elton Zheng, Olatunji Ruwase, Jeff Rasley, Jason Li, Junhua Wang, and Yuxiong He. 2019. Accelerating Large Scale Deep Learning Inference through DeepCPU at Microsoft. In *2019 USENIX Conference on Operational Machine Learning, OpML 2019, Santa Clara, CA, USA, May 20, 2019.*, Bharath Ramsundar and Nisha Talagala (Eds.). USENIX Association, 5–7. https://www.usenix.org/conference/opml19/presentation/zhang-minjia

[77] Zhuoyao Zhang, Ludmila Cherkasova, and Boon Thau Loo. 2014. Optimizing cost and performance trade-offs for mapreduce job processing in the cloud. In *Network Operations and Management Symposium (NOMS), 2014 IEEE*. IEEE, 1–8.

Appendix: Artifact Description/Artifact Evaluation

SUMMARY OF THE EXPERIMENTS REPORTED

We ran Tensorflow Serving 1.5.0 on a cluster of 10 identical servers. For CPU experiments, the Tensorflow Serving is compiled without CUDA. For GPU experiments, Tensorflow Serving is compiled with CUDA 9.0 so that it will utilize both CPU and GPU. Each of our server is equipped with dual-sockets Intel(R) Xeon(R) CPU E5-2630 v4 @2.20GHz and four NVIDIA GeForce GTX 1080 Ti GPUs, 64 GB of memory, and connected through Infiniband. One sever is acting as client, one server is used as dispatch queue, and the rest are request processing severs.

ARTIFACT AVAILABILITY

Software Artifact Availability: All author-created software artifacts are maintained in a public repository under an OSI-approved license.

Hardware Artifact Availability: There are no author-created hardware artifacts.

Data Artifact Availability: There are no author-created data artifacts.

Proprietary Artifacts: None of the associated artifacts, author-created or otherwise, are proprietary.

List of URLs and/or DOIs where artifacts are available:

```
RRL: https://github.com/SC-RRL/RRL
Tensorflow Serving:
↪ https://github.com/tensorflow/serving/tree/r1.5
DeepRM: https://github.com/hongzimao/deeprm
CAPES: https://github.com/mlogic/capes-oss
```

BASELINE EXPERIMENTAL SETUP, AND MODIFICATIONS MADE FOR THE PAPER

Relevant hardware details: Each of our server is equipped with dual-sockets Intel(R) Xeon(R) CPU E5-2630 v4 @2.20GHz and four NVIDIA GeForce GTX 1080 Ti GPUs, 64 GB of memory, and connected through Infiniband.

Operating systems and versions: Ubuntu 16.04

Applications and versions: Tensorflow Serving 1.5.0

Libraries and versions: CUDA 9.0

Key algorithms: Subspace based reinforcement learning algorithm and machine learning model serving scheduling framework

Input datasets and versions: ImageNet

Paper Modifications: Tensorflow Serving: we performed instrumentations to Tensorflow Serving to support measuring runtime performance data to collect necessary measurements used in our algorithms. We release the code in RRL github. DeepRM: We changed its input and output size to make it compatible with Tensorflow Serving. CAPES: We changed the input and output size of its DQL-Daemon to make it compatible with Tensorflow Serving.

Output from scripts that gathers execution environment information.

```
+ lsb_release -a
No LSB modules are available.
Distributor ID:        Ubuntu
Description:        Ubuntu 16.04.5 LTS
Release:        16.04
Codename:        xenial
+ uname -a
Linux node06 4.4.0-143-generic #169-Ubuntu SMP Thu Feb
↪ 7 07:56:38 UTC 2019 x86_64 x86_64 x86_64 GNU/Linux
+ lscpu
Architecture:          x86_64
CPU op-mode(s):        32-bit, 64-bit
Byte Order:            Little Endian
CPU(s):                40
On-line CPU(s) list:   0-39
Thread(s) per core:    2
Core(s) per socket:    10
Socket(s):             2
NUMA node(s):          2
Vendor ID:             GenuineIntel
CPU family:            6
Model:                 79
Model name:            Intel(R) Xeon(R) CPU E5-2630 v4
↪ @ 2.20GHz
Stepping:              1
CPU MHz:               1200.289
CPU max MHz:           3100.0000
CPU min MHz:           1200.0000
BogoMIPS:              4401.65
Virtualization:        VT-x
L1d cache:             32K
L1i cache:             32K
L2 cache:              256K
L3 cache:              25600K
NUMA node0 CPU(s):     0-9,20-29
NUMA node1 CPU(s):     10-19,30-39
```

```
Flags:                fpu vme de pse tsc msr pae mce
↪  cx8 apic sep mtrr pge mca cmov pat pse36 clflush
↪  dts acpi mmx fxsr sse sse2 ss ht tm pbe syscall nx
↪  pdpe1gb rdtscp lm constant_tsc arch_perfmon pebs
↪  bts rep_good nopl xtopology nonstop_tsc aperfmperf
↪  pni pclmulqdq dtes64 monitor ds_cpl vmx smx est
↪  tm2 ssse3 sdbg fma cx16 xtpr pdcm pcid dca sse4_1
↪  sse4_2 x2apic movbe popcnt tsc_deadline_timer aes
↪  xsave avx f16c rdrand lahf_lm abm 3dnowprefetch
↪  epb invpcid_single intel_pt ssbd ibrs ibpb stibp
↪  kaiser tpr_shadow vnmi flexpriority ept vpid
↪  fsgsbase tsc_adjust bmi1 hle avx2 smep bmi2 erms
↪  invpcid rtm cqm rdseed adx smap xsaveopt cqm_llc
↪  cqm_occup_llc cqm_mbm_total cqm_mbm_local dtherm
↪  ida arat pln pts flush_l1d
+ cat /proc/meminfo
MemTotal:       65858696 kB
MemFree:        17758376 kB
MemAvailable:   64448196 kB
Buffers:          220056 kB
Cached:         46276540 kB
SwapCached:           352 kB
Active:         21514572 kB
Inactive:       25021620 kB
Active(anon):      31704 kB
Inactive(anon):    28652 kB
Active(file):   21482868 kB
Inactive(file): 24992968 kB
Unevictable:        3652 kB
Mlocked:            3652 kB
SwapTotal:      66994172 kB
SwapFree:       66993468 kB
Dirty:                0 kB
Writeback:            0 kB
AnonPages:         43060 kB
Mapped:            37404 kB
Shmem:             18336 kB
Slab:             851984 kB
SReclaimable:     711056 kB
SUnreclaim:       140928 kB
KernelStack:        8496 kB
PageTables:         5420 kB
NFS_Unstable:          0 kB
Bounce:                0 kB
WritebackTmp:          0 kB
CommitLimit:    99923520 kB
Committed_AS:     241368 kB
VmallocTotal:   34359738367 kB
VmallocUsed:           0 kB
VmallocChunk:          0 kB
HardwareCorrupted:     0 kB
AnonHugePages:         0 kB
CmaTotal:              0 kB
CmaFree:               0 kB
HugePages_Total:       0
HugePages_Free:        0
HugePages_Rsvd:        0
HugePages_Surp:        0
Hugepagesize:       2048 kB
DirectMap4k:    11863352 kB
DirectMap2M:    55132160 kB
DirectMap1G:     2097152 kB
+ inxi -F -c0
System:    Host: node06 Kernel: 4.4.0-143-generic
↪  x86_64 (64 bit)
           Console: tty 2 Distro: Ubuntu 16.04 xenial
Machine:   System: Supermicro product: SYS-1028GQ-TRT
↪  v: 123456789
           Mobo: Supermicro model: X10DGQ v: 1.00
           Bios: American Megatrends v: 2.0b date:
           ↪  05/16/2017
CPU(s):    2 Deca core Intel Xeon E5-2630 v4s
↪  (-HT-MCP-SMP-) cache: 51200 KB
           clock speeds: max: 3100 MHz 1: 1228 MHz 2:
           ↪  1274 MHz 3: 1228 MHz
           4: 1200 MHz 5: 1247 MHz 6: 1242 MHz 7: 1459
           ↪  MHz 8: 1200 MHz
           9: 1326 MHz 10: 1285 MHz 11: 1200 MHz 12:
           ↪  1200 MHz 13: 1200 MHz
           14: 1290 MHz 15: 1269 MHz 16: 1214 MHz 17:
           ↪  1200 MHz 18: 1276 MHz
           19: 1200 MHz 20: 1235 MHz 21: 1316 MHz 22:
           ↪  1279 MHz 23: 1221 MHz
           24: 1247 MHz 25: 1200 MHz 26: 1229 MHz 27:
           ↪  1300 MHz 28: 1200 MHz
           29: 1261 MHz 30: 1203 MHz 31: 1263 MHz 32:
           ↪  1200 MHz 33: 1225 MHz
           34: 1294 MHz 35: 1282 MHz 36: 1315 MHz 37:
           ↪  1284 MHz 38: 1270 MHz
           39: 1263 MHz 40: 1200 MHz
Graphics:  Card-1: NVIDIA Device 1b06
           Card-2: NVIDIA Device 1b06
           Card-3: ASPEED ASPEED Graphics Family
           Card-4: NVIDIA Device 1b06
           Card-5: NVIDIA Device 1b06
           Display Server: N/A driver: N/A
           tty size: 94x48 Advanced Data: N/A out of X
Audio:     Card 4x NVIDIA Device 10ef
           driver: snd_hda_intelsnd_hda_intelsnd_hda_
           ↪  intelsnd_hda_intel
           Sound: Advanced Linux Sound Architecture v:
           ↪  k4.4.0-143-generic
Network:   Card-1: Intel Ethernet Controller
↪  10-Gigabit X540-AT2 driver: ixgbe
           IF: enp4s0f0 state: up speed: 1000 Mbps
           ↪  duplex: full
           mac: ac:1f:6b:05:72:52
           Card-2: Intel Ethernet Controller
           ↪  10-Gigabit X540-AT2 driver: ixgbe
           IF: enp4s0f1 state: up speed: 10000 Mbps
           ↪  duplex: full
           mac: ac:1f:6b:05:72:53
```

```
           Card-3: Mellanox MT27520 Family [ConnectX-3
            ↪  Pro] driver: mlx4_core
           IF: ib0 state: up speed: N/A duplex: N/A
           mac: 80:00:02:08:fe:80:00:00:00:00:00:00:02
            ↪  4:8a:07:03:00:c3:f1:31
Drives:    HDD Total Size: 2920.6GB (7.9% used)
           ID-1: /dev/sdb model: Micron_5100_MTFD
            ↪  size: 1920.4GB
           ID-2: /dev/sda model: ST1000NX0313 size:
            ↪  1000.2GB
           ID-1: / size: 6.5T used: 136G (3%) fs: nfs4
            ↪  remote: stor:/schroot/
           ID-2: /tmp size: 1.7T used: 155G (10%) fs:
            ↪  ext4 dev: /dev/dm-0
           ID-3: swap-1 size: 68.60GB used: 0.00GB
            ↪  (0%) fs: swap dev: /dev/dm-1
RAID:      No RAID devices: /proc/mdstat, md_mod
↪  kernel module present
Sensors:   System Temperatures: cpu: 32.0C mobo: N/A
           Fan Speeds (in rpm): cpu: N/A
Info:      Processes: 486 Uptime: 22 days Memory:
↪  1593.0/64315.1MB
           Init: systemd Client: Shell (bash) inxi:
            ↪  2.2.35
+ lsblk -a
NAME                    MAJ:MIN RM   SIZE RO TYPE
↪  MOUNTPOINT
sda                       8:0    0 931.5G  0 disk
sdb                       8:16   0   1.8T  0 disk
├─sdb1                    8:17   0   487M  0 part
├─sdb2                    8:18   0     1K  0 part
└─sdb5                    8:21   0   1.8T  0 part
  ├─gnode04--vg-root    252:0    0   1.7T  0 lvm  /data
  └─gnode04--vg-swap_1  252:1    0  63.9G  0 lvm  [SWAP]
loop0                     7:0    0         0 loop
loop1                     7:1    0         0 loop
loop2                     7:2    0         0 loop
loop3                     7:3    0         0 loop
loop4                     7:4    0         0 loop
loop5                     7:5    0         0 loop
loop6                     7:6    0         0 loop
loop7                     7:7    0         0 loop
+ lsscsi -s
[4:0:0:0]    disk    ATA      ST1000NX0313     SN02
↪  /dev/sda   1.00TB
[5:0:0:0]    disk    ATA      Micron_5100_MTFD U027
↪  /dev/sdb   1.92TB
+ nvidia-smi
Tue Apr  9 22:11:08 2019
+-----------------------------------------------------
↪  ------------------------+
| NVIDIA-SMI 418.39       Driver Version: 418.39
↪  CUDA Version: 10.1     |
|-------------------------------+----------------------
↪  ---+----------------------+
| GPU  Name        Persistence-M| Bus-Id        Disp.A
↪  | Volatile Uncorr. ECC |
| Fan  Temp  Perf  Pwr:Usage/Cap|         Memory-Usage
↪  | GPU-Util  Compute M. |
|===============================+======================
↪  ===+======================|
|   0  GeForce GTX 108...  Off  | 00000000:02:00.0 Off
↪  |                  N/A |
| 18%   31C    P0    60W / 250W |      0MiB / 11178MiB
↪  |      0%      Default |
+-------------------------------+----------------------
↪  ---+----------------------+
|   1  GeForce GTX 108...  Off  | 00000000:03:00.0 Off
↪  |                  N/A |
| 19%   26C    P0    59W / 250W |      0MiB / 11178MiB
↪  |      0%      Default |
+-------------------------------+----------------------
↪  ---+----------------------+
|   2  GeForce GTX 108...  Off  | 00000000:82:00.0 Off
↪  |                  N/A |
| 17%   28C    P0    58W / 250W |      0MiB / 11178MiB
↪  |      0%      Default |
+-------------------------------+----------------------
↪  ---+----------------------+
|   3  GeForce GTX 108...  Off  | 00000000:83:00.0 Off
↪  |                  N/A |
| 19%   27C    P0    59W / 250W |      0MiB / 11178MiB
↪  |      0%      Default |
+-------------------------------+----------------------
↪  ---+----------------------+

+-----------------------------------------------------
↪  ------------------------+
| Processes:
↪                GPU Memory |
|  GPU       PID   Type   Process name
↪                Usage      |
|=============================================
↪  ========================|
|  No running processes found
↪                           |
+-----------------------------------------------------
↪  ------------------------+

+ cat
+ lshw -short -quiet -sanitize
bash: lshw: command not found
+ lspci
00:00.0 Host bridge: Intel Corporation Xeon E7
↪  v4/Xeon E5 v4/Xeon E3 v4/Xeon D DMI2 (rev 01)
```

```
00:01.0 PCI bridge: Intel Corporation Xeon E7 v4/Xeon
↪  E5 v4/Xeon E3 v4/Xeon D PCI Express Root Port 1
↪  (rev 01)
00:02.0 PCI bridge: Intel Corporation Xeon E7 v4/Xeon
↪  E5 v4/Xeon E3 v4/Xeon D PCI Express Root Port 2
↪  (rev 01)
00:03.0 PCI bridge: Intel Corporation Xeon E7 v4/Xeon
↪  E5 v4/Xeon E3 v4/Xeon D PCI Express Root Port 3
↪  (rev 01)
00:04.0 System peripheral: Intel Corporation Xeon E7
↪  v4/Xeon E5 v4/Xeon E3 v4/Xeon D Crystal Beach DMA
↪  Channel 0 (rev 01)
00:04.1 System peripheral: Intel Corporation Xeon E7
↪  v4/Xeon E5 v4/Xeon E3 v4/Xeon D Crystal Beach DMA
↪  Channel 1 (rev 01)
00:04.2 System peripheral: Intel Corporation Xeon E7
↪  v4/Xeon E5 v4/Xeon E3 v4/Xeon D Crystal Beach DMA
↪  Channel 2 (rev 01)
00:04.3 System peripheral: Intel Corporation Xeon E7
↪  v4/Xeon E5 v4/Xeon E3 v4/Xeon D Crystal Beach DMA
↪  Channel 3 (rev 01)
00:04.4 System peripheral: Intel Corporation Xeon E7
↪  v4/Xeon E5 v4/Xeon E3 v4/Xeon D Crystal Beach DMA
↪  Channel 4 (rev 01)
00:04.5 System peripheral: Intel Corporation Xeon E7
↪  v4/Xeon E5 v4/Xeon E3 v4/Xeon D Crystal Beach DMA
↪  Channel 5 (rev 01)
00:04.6 System peripheral: Intel Corporation Xeon E7
↪  v4/Xeon E5 v4/Xeon E3 v4/Xeon D Crystal Beach DMA
↪  Channel 6 (rev 01)
00:04.7 System peripheral: Intel Corporation Xeon E7
↪  v4/Xeon E5 v4/Xeon E3 v4/Xeon D Crystal Beach DMA
↪  Channel 7 (rev 01)
00:05.0 System peripheral: Intel Corporation Xeon E7
↪  v4/Xeon E5 v4/Xeon E3 v4/Xeon D
↪  Map/VTd_Misc/System Management (rev 01)
00:05.1 System peripheral: Intel Corporation Xeon E7
↪  v4/Xeon E5 v4/Xeon E3 v4/Xeon D IIO Hot Plug (rev
↪  01)
00:05.2 System peripheral: Intel Corporation Xeon E7
↪  v4/Xeon E5 v4/Xeon E3 v4/Xeon D IIO RAS/Control
↪  Status/Global Errors (rev 01)
00:05.4 PIC: Intel Corporation Xeon E7 v4/Xeon E5
↪  v4/Xeon E3 v4/Xeon D I/O APIC (rev 01)
00:11.0 Unassigned class [ff00]: Intel Corporation
↪  C610/X99 series chipset SPSR (rev 05)
00:11.4 SATA controller: Intel Corporation C610/X99
↪  series chipset sSATA Controller [AHCI mode] (rev
↪  05)
00:14.0 USB controller: Intel Corporation C610/X99
↪  series chipset USB xHCI Host Controller (rev 05)
00:16.0 Communication controller: Intel Corporation
↪  C610/X99 series chipset MEI Controller #1 (rev 05)
00:16.1 Communication controller: Intel Corporation
↪  C610/X99 series chipset MEI Controller #2 (rev 05)
00:1a.0 USB controller: Intel Corporation C610/X99
↪  series chipset USB Enhanced Host Controller #2
↪  (rev 05)
00:1c.0 PCI bridge: Intel Corporation C610/X99 series
↪  chipset PCI Express Root Port #1 (rev d5)
00:1c.4 PCI bridge: Intel Corporation C610/X99 series
↪  chipset PCI Express Root Port #5 (rev d5)
00:1d.0 USB controller: Intel Corporation C610/X99
↪  series chipset USB Enhanced Host Controller #1
↪  (rev 05)
00:1f.0 ISA bridge: Intel Corporation C610/X99 series
↪  chipset LPC Controller (rev 05)
00:1f.2 SATA controller: Intel Corporation C610/X99
↪  series chipset 6-Port SATA Controller [AHCI mode]
↪  (rev 05)
00:1f.3 SMBus: Intel Corporation C610/X99 series
↪  chipset SMBus Controller (rev 05)
02:00.0 VGA compatible controller: NVIDIA Corporation
↪  Device 1b06 (rev a1)
02:00.1 Audio device: NVIDIA Corporation Device 10ef
↪  (rev a1)
03:00.0 VGA compatible controller: NVIDIA Corporation
↪  Device 1b06 (rev a1)
03:00.1 Audio device: NVIDIA Corporation Device 10ef
↪  (rev a1)
04:00.0 Ethernet controller: Intel Corporation
↪  Ethernet Controller 10-Gigabit X540-AT2 (rev 01)
04:00.1 Ethernet controller: Intel Corporation
↪  Ethernet Controller 10-Gigabit X540-AT2 (rev 01)
05:00.0 PCI bridge: ASPEED Technology, Inc. AST1150
↪  PCI-to-PCI Bridge (rev 03)
06:00.0 VGA compatible controller: ASPEED Technology,
↪  Inc. ASPEED Graphics Family (rev 30)
7f:08.0 System peripheral: Intel Corporation Xeon E7
↪  v4/Xeon E5 v4/Xeon E3 v4/Xeon D QPI Link 0 (rev
↪  01)
7f:08.2 Performance counters: Intel Corporation Xeon
↪  E7 v4/Xeon E5 v4/Xeon E3 v4/Xeon D QPI Link 0 (rev
↪  01)
7f:08.3 System peripheral: Intel Corporation Xeon E7
↪  v4/Xeon E5 v4/Xeon E3 v4/Xeon D QPI Link 0 (rev
↪  01)
7f:09.0 System peripheral: Intel Corporation Xeon E7
↪  v4/Xeon E5 v4/Xeon E3 v4/Xeon D QPI Link 1 (rev
↪  01)
7f:09.2 Performance counters: Intel Corporation Xeon
↪  E7 v4/Xeon E5 v4/Xeon E3 v4/Xeon D QPI Link 1 (rev
↪  01)
7f:09.3 System peripheral: Intel Corporation Xeon E7
↪  v4/Xeon E5 v4/Xeon E3 v4/Xeon D QPI Link 1 (rev
↪  01)
7f:0b.0 System peripheral: Intel Corporation Xeon E7
↪  v4/Xeon E5 v4/Xeon E3 v4/Xeon D R3 QPI Link 0/1
↪  (rev 01)
```

```
7f:0b.1 Performance counters: Intel Corporation Xeon
↪  E7 v4/Xeon E5 v4/Xeon E3 v4/Xeon D R3 QPI Link 0/1
↪  (rev 01)
7f:0b.2 Performance counters: Intel Corporation Xeon
↪  E7 v4/Xeon E5 v4/Xeon E3 v4/Xeon D R3 QPI Link 0/1
↪  (rev 01)
7f:0b.3 System peripheral: Intel Corporation Xeon E7
↪  v4/Xeon E5 v4/Xeon E3 v4/Xeon D R3 QPI Link Debug
↪  (rev 01)
7f:0c.0 System peripheral: Intel Corporation Xeon E7
↪  v4/Xeon E5 v4/Xeon E3 v4/Xeon D Caching Agent (rev
↪  01)
7f:0c.1 System peripheral: Intel Corporation Xeon E7
↪  v4/Xeon E5 v4/Xeon E3 v4/Xeon D Caching Agent (rev
↪  01)
7f:0c.2 System peripheral: Intel Corporation Xeon E7
↪  v4/Xeon E5 v4/Xeon E3 v4/Xeon D Caching Agent (rev
↪  01)
7f:0c.3 System peripheral: Intel Corporation Xeon E7
↪  v4/Xeon E5 v4/Xeon E3 v4/Xeon D Caching Agent (rev
↪  01)
7f:0c.4 System peripheral: Intel Corporation Xeon E7
↪  v4/Xeon E5 v4/Xeon E3 v4/Xeon D Caching Agent (rev
↪  01)
7f:0c.5 System peripheral: Intel Corporation Xeon E7
↪  v4/Xeon E5 v4/Xeon E3 v4/Xeon D Caching Agent (rev
↪  01)
7f:0c.6 System peripheral: Intel Corporation Xeon E7
↪  v4/Xeon E5 v4/Xeon E3 v4/Xeon D Caching Agent (rev
↪  01)
7f:0c.7 System peripheral: Intel Corporation Xeon E7
↪  v4/Xeon E5 v4/Xeon E3 v4/Xeon D Caching Agent (rev
↪  01)
7f:0d.0 System peripheral: Intel Corporation Xeon E7
↪  v4/Xeon E5 v4/Xeon E3 v4/Xeon D Caching Agent (rev
↪  01)
7f:0d.1 System peripheral: Intel Corporation Xeon E7
↪  v4/Xeon E5 v4/Xeon E3 v4/Xeon D Caching Agent (rev
↪  01)
7f:0f.0 System peripheral: Intel Corporation Xeon E7
↪  v4/Xeon E5 v4/Xeon E3 v4/Xeon D Caching Agent (rev
↪  01)
7f:0f.1 System peripheral: Intel Corporation Xeon E7
↪  v4/Xeon E5 v4/Xeon E3 v4/Xeon D Caching Agent (rev
↪  01)
7f:0f.4 System peripheral: Intel Corporation Xeon E7
↪  v4/Xeon E5 v4/Xeon E3 v4/Xeon D Caching Agent (rev
↪  01)
7f:0f.5 System peripheral: Intel Corporation Xeon E7
↪  v4/Xeon E5 v4/Xeon E3 v4/Xeon D Caching Agent (rev
↪  01)
7f:0f.6 System peripheral: Intel Corporation Xeon E7
↪  v4/Xeon E5 v4/Xeon E3 v4/Xeon D Caching Agent (rev
↪  01)
7f:10.0 System peripheral: Intel Corporation Xeon E7
↪  v4/Xeon E5 v4/Xeon E3 v4/Xeon D R2PCIe Agent (rev
↪  01)
7f:10.1 Performance counters: Intel Corporation Xeon
↪  E7 v4/Xeon E5 v4/Xeon E3 v4/Xeon D R2PCIe Agent
↪  (rev 01)
7f:10.5 System peripheral: Intel Corporation Xeon E7
↪  v4/Xeon E5 v4/Xeon E3 v4/Xeon D Ubox (rev 01)
7f:10.6 Performance counters: Intel Corporation Xeon
↪  E7 v4/Xeon E5 v4/Xeon E3 v4/Xeon D Ubox (rev 01)
7f:10.7 System peripheral: Intel Corporation Xeon E7
↪  v4/Xeon E5 v4/Xeon E3 v4/Xeon D Ubox (rev 01)
7f:12.0 System peripheral: Intel Corporation Xeon E7
↪  v4/Xeon E5 v4/Xeon E3 v4/Xeon D Home Agent 0 (rev
↪  01)
7f:12.1 Performance counters: Intel Corporation Xeon
↪  E7 v4/Xeon E5 v4/Xeon E3 v4/Xeon D Home Agent 0
↪  (rev 01)
7f:13.0 System peripheral: Intel Corporation Xeon E7
↪  v4/Xeon E5 v4/Xeon E3 v4/Xeon D Memory Controller
↪  0 - Target Address/Thermal/RAS (rev 01)
7f:13.1 System peripheral: Intel Corporation Xeon E7
↪  v4/Xeon E5 v4/Xeon E3 v4/Xeon D Memory Controller
↪  0 - Target Address/Thermal/RAS (rev 01)
7f:13.2 System peripheral: Intel Corporation Xeon E7
↪  v4/Xeon E5 v4/Xeon E3 v4/Xeon D Memory Controller
↪  0 - Channel Target Address Decoder (rev 01)
7f:13.3 System peripheral: Intel Corporation Xeon E7
↪  v4/Xeon E5 v4/Xeon E3 v4/Xeon D Memory Controller
↪  0 - Channel Target Address Decoder (rev 01)
7f:13.4 System peripheral: Intel Corporation Xeon E7
↪  v4/Xeon E5 v4/Xeon E3 v4/Xeon D Memory Controller
↪  0 - Channel Target Address Decoder (rev 01)
7f:13.5 System peripheral: Intel Corporation Xeon E7
↪  v4/Xeon E5 v4/Xeon E3 v4/Xeon D Memory Controller
↪  0 - Channel Target Address Decoder (rev 01)
7f:13.6 System peripheral: Intel Corporation Xeon E7
↪  v4/Xeon E5 v4/Xeon E3 v4/Xeon D DDRIO Channel 0/1
↪  Broadcast (rev 01)
7f:13.7 System peripheral: Intel Corporation Xeon E7
↪  v4/Xeon E5 v4/Xeon E3 v4/Xeon D DDRIO Global
↪  Broadcast (rev 01)
7f:14.0 System peripheral: Intel Corporation Xeon E7
↪  v4/Xeon E5 v4/Xeon E3 v4/Xeon D Memory Controller
↪  0 - Channel 0 Thermal Control (rev 01)
7f:14.1 System peripheral: Intel Corporation Xeon E7
↪  v4/Xeon E5 v4/Xeon E3 v4/Xeon D Memory Controller
↪  0 - Channel 1 Thermal Control (rev 01)
7f:14.2 System peripheral: Intel Corporation Xeon E7
↪  v4/Xeon E5 v4/Xeon E3 v4/Xeon D Memory Controller
↪  0 - Channel 0 Error (rev 01)
7f:14.3 System peripheral: Intel Corporation Xeon E7
↪  v4/Xeon E5 v4/Xeon E3 v4/Xeon D Memory Controller
↪  0 - Channel 1 Error (rev 01)
7f:14.4 System peripheral: Intel Corporation Xeon E7
↪  v4/Xeon E5 v4/Xeon E3 v4/Xeon D DDRIO Channel 0/1
↪  Interface (rev 01)
```

```
7f:14.5 System peripheral: Intel Corporation Xeon E7
↪  v4/Xeon E5 v4/Xeon E3 v4/Xeon D DDRIO Channel 0/1
↪  Interface (rev 01)
7f:14.6 System peripheral: Intel Corporation Xeon E7
↪  v4/Xeon E5 v4/Xeon E3 v4/Xeon D DDRIO Channel 0/1
↪  Interface (rev 01)
7f:14.7 System peripheral: Intel Corporation Xeon E7
↪  v4/Xeon E5 v4/Xeon E3 v4/Xeon D DDRIO Channel 0/1
↪  Interface (rev 01)
7f:15.0 System peripheral: Intel Corporation Xeon E7
↪  v4/Xeon E5 v4/Xeon E3 v4/Xeon D Memory Controller
↪  0 - Channel 2 Thermal Control (rev 01)
7f:15.1 System peripheral: Intel Corporation Xeon E7
↪  v4/Xeon E5 v4/Xeon E3 v4/Xeon D Memory Controller
↪  0 - Channel 3 Thermal Control (rev 01)
7f:15.2 System peripheral: Intel Corporation Xeon E7
↪  v4/Xeon E5 v4/Xeon E3 v4/Xeon D Memory Controller
↪  0 - Channel 2 Error (rev 01)
7f:15.3 System peripheral: Intel Corporation Xeon E7
↪  v4/Xeon E5 v4/Xeon E3 v4/Xeon D Memory Controller
↪  0 - Channel 3 Error (rev 01)
7f:16.0 System peripheral: Intel Corporation Xeon E7
↪  v4/Xeon E5 v4/Xeon E3 v4/Xeon D Target
↪  Address/Thermal/RAS (rev 01)
7f:16.6 System peripheral: Intel Corporation Xeon E7
↪  v4/Xeon E5 v4/Xeon E3 v4/Xeon D DDRIO Channel 2/3
↪  Broadcast (rev 01)
7f:16.7 System peripheral: Intel Corporation Xeon E7
↪  v4/Xeon E5 v4/Xeon E3 v4/Xeon D DDRIO Global
↪  Broadcast (rev 01)
7f:17.0 System peripheral: Intel Corporation Xeon E7
↪  v4/Xeon E5 v4/Xeon E3 v4/Xeon D Memory Controller
↪  1 - Channel 0 Thermal Control (rev 01)
7f:17.4 System peripheral: Intel Corporation Xeon E7
↪  v4/Xeon E5 v4/Xeon E3 v4/Xeon D DDRIO Channel 2/3
↪  Interface (rev 01)
7f:17.5 System peripheral: Intel Corporation Xeon E7
↪  v4/Xeon E5 v4/Xeon E3 v4/Xeon D DDRIO Channel 2/3
↪  Interface (rev 01)
7f:17.6 System peripheral: Intel Corporation Xeon E7
↪  v4/Xeon E5 v4/Xeon E3 v4/Xeon D DDRIO Channel 2/3
↪  Interface (rev 01)
7f:17.7 System peripheral: Intel Corporation Xeon E7
↪  v4/Xeon E5 v4/Xeon E3 v4/Xeon D DDRIO Channel 2/3
↪  Interface (rev 01)
7f:1e.0 System peripheral: Intel Corporation Xeon E7
↪  v4/Xeon E5 v4/Xeon E3 v4/Xeon D Power Control Unit
↪  (rev 01)
7f:1e.1 System peripheral: Intel Corporation Xeon E7
↪  v4/Xeon E5 v4/Xeon E3 v4/Xeon D Power Control Unit
↪  (rev 01)
7f:1e.2 System peripheral: Intel Corporation Xeon E7
↪  v4/Xeon E5 v4/Xeon E3 v4/Xeon D Power Control Unit
↪  (rev 01)
7f:1e.3 System peripheral: Intel Corporation Xeon E7
↪  v4/Xeon E5 v4/Xeon E3 v4/Xeon D Power Control Unit
↪  (rev 01)
7f:1e.4 System peripheral: Intel Corporation Xeon E7
↪  v4/Xeon E5 v4/Xeon E3 v4/Xeon D Power Control Unit
↪  (rev 01)
7f:1f.0 System peripheral: Intel Corporation Xeon E7
↪  v4/Xeon E5 v4/Xeon E3 v4/Xeon D Power Control Unit
↪  (rev 01)
7f:1f.2 System peripheral: Intel Corporation Xeon E7
↪  v4/Xeon E5 v4/Xeon E3 v4/Xeon D Power Control Unit
↪  (rev 01)
80:01.0 PCI bridge: Intel Corporation Xeon E7 v4/Xeon
↪  E5 v4/Xeon E3 v4/Xeon D PCI Express Root Port 1
↪  (rev 01)
80:02.0 PCI bridge: Intel Corporation Xeon E7 v4/Xeon
↪  E5 v4/Xeon E3 v4/Xeon D PCI Express Root Port 2
↪  (rev 01)
80:03.0 PCI bridge: Intel Corporation Xeon E7 v4/Xeon
↪  E5 v4/Xeon E3 v4/Xeon D PCI Express Root Port 3
↪  (rev 01)
80:04.0 System peripheral: Intel Corporation Xeon E7
↪  v4/Xeon E5 v4/Xeon E3 v4/Xeon D Crystal Beach DMA
↪  Channel 0 (rev 01)
80:04.1 System peripheral: Intel Corporation Xeon E7
↪  v4/Xeon E5 v4/Xeon E3 v4/Xeon D Crystal Beach DMA
↪  Channel 1 (rev 01)
80:04.2 System peripheral: Intel Corporation Xeon E7
↪  v4/Xeon E5 v4/Xeon E3 v4/Xeon D Crystal Beach DMA
↪  Channel 2 (rev 01)
80:04.3 System peripheral: Intel Corporation Xeon E7
↪  v4/Xeon E5 v4/Xeon E3 v4/Xeon D Crystal Beach DMA
↪  Channel 3 (rev 01)
80:04.4 System peripheral: Intel Corporation Xeon E7
↪  v4/Xeon E5 v4/Xeon E3 v4/Xeon D Crystal Beach DMA
↪  Channel 4 (rev 01)
80:04.5 System peripheral: Intel Corporation Xeon E7
↪  v4/Xeon E5 v4/Xeon E3 v4/Xeon D Crystal Beach DMA
↪  Channel 5 (rev 01)
80:04.6 System peripheral: Intel Corporation Xeon E7
↪  v4/Xeon E5 v4/Xeon E3 v4/Xeon D Crystal Beach DMA
↪  Channel 6 (rev 01)
80:04.7 System peripheral: Intel Corporation Xeon E7
↪  v4/Xeon E5 v4/Xeon E3 v4/Xeon D Crystal Beach DMA
↪  Channel 7 (rev 01)
80:05.0 System peripheral: Intel Corporation Xeon E7
↪  v4/Xeon E5 v4/Xeon E3 v4/Xeon D
↪  Map/VTd_Misc/System Management (rev 01)
80:05.1 System peripheral: Intel Corporation Xeon E7
↪  v4/Xeon E5 v4/Xeon E3 v4/Xeon D IIO Hot Plug (rev
↪  01)
80:05.2 System peripheral: Intel Corporation Xeon E7
↪  v4/Xeon E5 v4/Xeon E3 v4/Xeon D IIO RAS/Control
↪  Status/Global Errors (rev 01)
80:05.4 PIC: Intel Corporation Xeon E7 v4/Xeon E5
↪  v4/Xeon E3 v4/Xeon D I/O APIC (rev 01)
81:00.0 Network controller: Mellanox Technologies
↪  MT27520 Family [ConnectX-3 Pro]
```

```
82:00.0 VGA compatible controller: NVIDIA Corporation
↪  Device 1b06 (rev a1)
82:00.1 Audio device: NVIDIA Corporation Device 10ef
↪  (rev a1)
83:00.0 VGA compatible controller: NVIDIA Corporation
↪  Device 1b06 (rev a1)
83:00.1 Audio device: NVIDIA Corporation Device 10ef
↪  (rev a1)
ff:08.0 System peripheral: Intel Corporation Xeon E7
↪  v4/Xeon E5 v4/Xeon E3 v4/Xeon D QPI Link 0 (rev
↪  01)
ff:08.2 Performance counters: Intel Corporation Xeon
↪  E7 v4/Xeon E5 v4/Xeon E3 v4/Xeon D QPI Link 0 (rev
↪  01)
ff:08.3 System peripheral: Intel Corporation Xeon E7
↪  v4/Xeon E5 v4/Xeon E3 v4/Xeon D QPI Link 0 (rev
↪  01)
ff:09.0 System peripheral: Intel Corporation Xeon E7
↪  v4/Xeon E5 v4/Xeon E3 v4/Xeon D QPI Link 1 (rev
↪  01)
ff:09.2 Performance counters: Intel Corporation Xeon
↪  E7 v4/Xeon E5 v4/Xeon E3 v4/Xeon D QPI Link 1 (rev
↪  01)
ff:09.3 System peripheral: Intel Corporation Xeon E7
↪  v4/Xeon E5 v4/Xeon E3 v4/Xeon D QPI Link 1 (rev
↪  01)
ff:0b.0 System peripheral: Intel Corporation Xeon E7
↪  v4/Xeon E5 v4/Xeon E3 v4/Xeon D R3 QPI Link 0/1
↪  (rev 01)
ff:0b.1 Performance counters: Intel Corporation Xeon
↪  E7 v4/Xeon E5 v4/Xeon E3 v4/Xeon D R3 QPI Link 0/1
↪  (rev 01)
ff:0b.2 Performance counters: Intel Corporation Xeon
↪  E7 v4/Xeon E5 v4/Xeon E3 v4/Xeon D R3 QPI Link 0/1
↪  (rev 01)
ff:0b.3 System peripheral: Intel Corporation Xeon E7
↪  v4/Xeon E5 v4/Xeon E3 v4/Xeon D R3 QPI Link Debug
↪  (rev 01)
ff:0c.0 System peripheral: Intel Corporation Xeon E7
↪  v4/Xeon E5 v4/Xeon E3 v4/Xeon D Caching Agent (rev
↪  01)
ff:0c.1 System peripheral: Intel Corporation Xeon E7
↪  v4/Xeon E5 v4/Xeon E3 v4/Xeon D Caching Agent (rev
↪  01)
ff:0c.2 System peripheral: Intel Corporation Xeon E7
↪  v4/Xeon E5 v4/Xeon E3 v4/Xeon D Caching Agent (rev
↪  01)
ff:0c.3 System peripheral: Intel Corporation Xeon E7
↪  v4/Xeon E5 v4/Xeon E3 v4/Xeon D Caching Agent (rev
↪  01)
ff:0c.4 System peripheral: Intel Corporation Xeon E7
↪  v4/Xeon E5 v4/Xeon E3 v4/Xeon D Caching Agent (rev
↪  01)
ff:0c.5 System peripheral: Intel Corporation Xeon E7
↪  v4/Xeon E5 v4/Xeon E3 v4/Xeon D Caching Agent (rev
↪  01)
ff:0c.6 System peripheral: Intel Corporation Xeon E7
↪  v4/Xeon E5 v4/Xeon E3 v4/Xeon D Caching Agent (rev
↪  01)
ff:0c.7 System peripheral: Intel Corporation Xeon E7
↪  v4/Xeon E5 v4/Xeon E3 v4/Xeon D Caching Agent (rev
↪  01)
ff:0d.0 System peripheral: Intel Corporation Xeon E7
↪  v4/Xeon E5 v4/Xeon E3 v4/Xeon D Caching Agent (rev
↪  01)
ff:0d.1 System peripheral: Intel Corporation Xeon E7
↪  v4/Xeon E5 v4/Xeon E3 v4/Xeon D Caching Agent (rev
↪  01)
ff:0f.0 System peripheral: Intel Corporation Xeon E7
↪  v4/Xeon E5 v4/Xeon E3 v4/Xeon D Caching Agent (rev
↪  01)
ff:0f.1 System peripheral: Intel Corporation Xeon E7
↪  v4/Xeon E5 v4/Xeon E3 v4/Xeon D Caching Agent (rev
↪  01)
ff:0f.4 System peripheral: Intel Corporation Xeon E7
↪  v4/Xeon E5 v4/Xeon E3 v4/Xeon D Caching Agent (rev
↪  01)
ff:0f.5 System peripheral: Intel Corporation Xeon E7
↪  v4/Xeon E5 v4/Xeon E3 v4/Xeon D Caching Agent (rev
↪  01)
ff:0f.6 System peripheral: Intel Corporation Xeon E7
↪  v4/Xeon E5 v4/Xeon E3 v4/Xeon D Caching Agent (rev
↪  01)
ff:10.0 System peripheral: Intel Corporation Xeon E7
↪  v4/Xeon E5 v4/Xeon E3 v4/Xeon D R2PCIe Agent (rev
↪  01)
ff:10.1 Performance counters: Intel Corporation Xeon
↪  E7 v4/Xeon E5 v4/Xeon E3 v4/Xeon D R2PCIe Agent
↪  (rev 01)
ff:10.5 System peripheral: Intel Corporation Xeon E7
↪  v4/Xeon E5 v4/Xeon E3 v4/Xeon D Ubox (rev 01)
ff:10.6 Performance counters: Intel Corporation Xeon
↪  E7 v4/Xeon E5 v4/Xeon E3 v4/Xeon D Ubox (rev 01)
ff:10.7 System peripheral: Intel Corporation Xeon E7
↪  v4/Xeon E5 v4/Xeon E3 v4/Xeon D Ubox (rev 01)
ff:12.0 System peripheral: Intel Corporation Xeon E7
↪  v4/Xeon E5 v4/Xeon E3 v4/Xeon D Home Agent 0 (rev
↪  01)
ff:12.1 Performance counters: Intel Corporation Xeon
↪  E7 v4/Xeon E5 v4/Xeon E3 v4/Xeon D Home Agent 0
↪  (rev 01)
ff:13.0 System peripheral: Intel Corporation Xeon E7
↪  v4/Xeon E5 v4/Xeon E3 v4/Xeon D Memory Controller
↪  0 - Target Address/Thermal/RAS (rev 01)
ff:13.1 System peripheral: Intel Corporation Xeon E7
↪  v4/Xeon E5 v4/Xeon E3 v4/Xeon D Memory Controller
↪  0 - Target Address/Thermal/RAS (rev 01)
ff:13.2 System peripheral: Intel Corporation Xeon E7
↪  v4/Xeon E5 v4/Xeon E3 v4/Xeon D Memory Controller
↪  0 - Channel Target Address Decoder (rev 01)
```

```
ff:13.3 System peripheral: Intel Corporation Xeon E7
↪  v4/Xeon E5 v4/Xeon E3 v4/Xeon D Memory Controller
↪  0 - Channel Target Address Decoder (rev 01)
ff:13.4 System peripheral: Intel Corporation Xeon E7
↪  v4/Xeon E5 v4/Xeon E3 v4/Xeon D Memory Controller
↪  0 - Channel Target Address Decoder (rev 01)
ff:13.5 System peripheral: Intel Corporation Xeon E7
↪  v4/Xeon E5 v4/Xeon E3 v4/Xeon D Memory Controller
↪  0 - Channel Target Address Decoder (rev 01)
ff:13.6 System peripheral: Intel Corporation Xeon E7
↪  v4/Xeon E5 v4/Xeon E3 v4/Xeon D DDRIO Channel 0/1
↪  Broadcast (rev 01)
ff:13.7 System peripheral: Intel Corporation Xeon E7
↪  v4/Xeon E5 v4/Xeon E3 v4/Xeon D DDRIO Global
↪  Broadcast (rev 01)
ff:14.0 System peripheral: Intel Corporation Xeon E7
↪  v4/Xeon E5 v4/Xeon E3 v4/Xeon D Memory Controller
↪  0 - Channel 0 Thermal Control (rev 01)
ff:14.1 System peripheral: Intel Corporation Xeon E7
↪  v4/Xeon E5 v4/Xeon E3 v4/Xeon D Memory Controller
↪  0 - Channel 1 Thermal Control (rev 01)
ff:14.2 System peripheral: Intel Corporation Xeon E7
↪  v4/Xeon E5 v4/Xeon E3 v4/Xeon D Memory Controller
↪  0 - Channel 0 Error (rev 01)
ff:14.3 System peripheral: Intel Corporation Xeon E7
↪  v4/Xeon E5 v4/Xeon E3 v4/Xeon D Memory Controller
↪  0 - Channel 1 Error (rev 01)
ff:14.4 System peripheral: Intel Corporation Xeon E7
↪  v4/Xeon E5 v4/Xeon E3 v4/Xeon D DDRIO Channel 0/1
↪  Interface (rev 01)
ff:14.5 System peripheral: Intel Corporation Xeon E7
↪  v4/Xeon E5 v4/Xeon E3 v4/Xeon D DDRIO Channel 0/1
↪  Interface (rev 01)
ff:14.6 System peripheral: Intel Corporation Xeon E7
↪  v4/Xeon E5 v4/Xeon E3 v4/Xeon D DDRIO Channel 0/1
↪  Interface (rev 01)
ff:14.7 System peripheral: Intel Corporation Xeon E7
↪  v4/Xeon E5 v4/Xeon E3 v4/Xeon D DDRIO Channel 0/1
↪  Interface (rev 01)
ff:15.0 System peripheral: Intel Corporation Xeon E7
↪  v4/Xeon E5 v4/Xeon E3 v4/Xeon D Memory Controller
↪  0 - Channel 2 Thermal Control (rev 01)
ff:15.1 System peripheral: Intel Corporation Xeon E7
↪  v4/Xeon E5 v4/Xeon E3 v4/Xeon D Memory Controller
↪  0 - Channel 3 Thermal Control (rev 01)
ff:15.2 System peripheral: Intel Corporation Xeon E7
↪  v4/Xeon E5 v4/Xeon E3 v4/Xeon D Memory Controller
↪  0 - Channel 2 Error (rev 01)
ff:15.3 System peripheral: Intel Corporation Xeon E7
↪  v4/Xeon E5 v4/Xeon E3 v4/Xeon D Memory Controller
↪  0 - Channel 3 Error (rev 01)
ff:16.0 System peripheral: Intel Corporation Xeon E7
↪  v4/Xeon E5 v4/Xeon E3 v4/Xeon D Target
↪  Address/Thermal/RAS (rev 01)
ff:16.6 System peripheral: Intel Corporation Xeon E7
↪  v4/Xeon E5 v4/Xeon E3 v4/Xeon D DDRIO Channel 2/3
↪  Broadcast (rev 01)
ff:16.7 System peripheral: Intel Corporation Xeon E7
↪  v4/Xeon E5 v4/Xeon E3 v4/Xeon D DDRIO Global
↪  Broadcast (rev 01)
ff:17.0 System peripheral: Intel Corporation Xeon E7
↪  v4/Xeon E5 v4/Xeon E3 v4/Xeon D Memory Controller
↪  1 - Channel 0 Thermal Control (rev 01)
ff:17.4 System peripheral: Intel Corporation Xeon E7
↪  v4/Xeon E5 v4/Xeon E3 v4/Xeon D DDRIO Channel 2/3
↪  Interface (rev 01)
ff:17.5 System peripheral: Intel Corporation Xeon E7
↪  v4/Xeon E5 v4/Xeon E3 v4/Xeon D DDRIO Channel 2/3
↪  Interface (rev 01)
ff:17.6 System peripheral: Intel Corporation Xeon E7
↪  v4/Xeon E5 v4/Xeon E3 v4/Xeon D DDRIO Channel 2/3
↪  Interface (rev 01)
ff:17.7 System peripheral: Intel Corporation Xeon E7
↪  v4/Xeon E5 v4/Xeon E3 v4/Xeon D DDRIO Channel 2/3
↪  Interface (rev 01)
ff:1e.0 System peripheral: Intel Corporation Xeon E7
↪  v4/Xeon E5 v4/Xeon E3 v4/Xeon D Power Control Unit
↪  (rev 01)
ff:1e.1 System peripheral: Intel Corporation Xeon E7
↪  v4/Xeon E5 v4/Xeon E3 v4/Xeon D Power Control Unit
↪  (rev 01)
ff:1e.2 System peripheral: Intel Corporation Xeon E7
↪  v4/Xeon E5 v4/Xeon E3 v4/Xeon D Power Control Unit
↪  (rev 01)
ff:1e.3 System peripheral: Intel Corporation Xeon E7
↪  v4/Xeon E5 v4/Xeon E3 v4/Xeon D Power Control Unit
↪  (rev 01)
ff:1e.4 System peripheral: Intel Corporation Xeon E7
↪  v4/Xeon E5 v4/Xeon E3 v4/Xeon D Power Control Unit
↪  (rev 01)
ff:1f.0 System peripheral: Intel Corporation Xeon E7
↪  v4/Xeon E5 v4/Xeon E3 v4/Xeon D Power Control Unit
↪  (rev 01)
ff:1f.2 System peripheral: Intel Corporation Xeon E7
↪  v4/Xeon E5 v4/Xeon E3 v4/Xeon D Power Control Unit
↪  (rev 01)
```

ARTIFACT EVALUATION

Verification and validation studies: We validated our approach through both theoretical proofs and experimental evaluations. The experimental evaluation includes extensive performance comparison, sensitive analysis, different practical scenarios. Specifically, we compare our approach with 2 state-of-the-art approaches in the following aspect (i) effectiveness in terms of minimizing latency; (ii) robustness in dynamic workload; (iii) strict SLO guarantee; (iv) effectiveness of meeting SLO while minimizing resource usage. We used 3 popular applications, 2 non-exponential request arrival workloads, and performed extensive experiments on both CPU and GPU clusters. The experiments of baseline approaches are conducted in the same environment.

Accuracy and precision of timings: Our performance data is collected from a build-in monitor in Tensorflow Serving. We use C++ 11 chrono steady_clock APIs to get time. Though the precision may

vary on different platforms, it generally has the precision of 1 ns on Linux.

Used manufactured solutions or spectral properties: None

Quantified the sensitivity of results to initial conditions and/or parameters of the computational environment: Our algorithm is not sensitive to initial conditions, but the system randomness might slightly change the results.

Controls, statistics, or other steps taken to make the measurements and analyses robust to variability and unknowns in the system. We perform each experiment multiple times. For experiments with random process (e.g., with non-exponential arrival process), we run the experiments long enough, i.e., stop the experiment after we observe statistical stability in results.